AD NUMBER

AD875026

LIMITATION CHANGES

TO:

Approved for public release; distribution is unlimited.

FROM:

Distribution authorized to U.S. Gov't. agencies and their contractors; Critical Technology; 22 JUL 1970. Other requests shall be referred to Defense Advanced Research Projects Agency, Attn: TIO, 675 North Randolph Street, Washington, DC 22203-2114. This document contains export-controlled technical data.

AUTHORITY

USAF ltr, 25 Jan 1972

AFTAC Project No. VELA/T/0701/B/ASD

NOISE STUDY FOR TFO EXTENDED SHORT-PERIOD ARRAY

Technical Report No. 5

SEISMIC ARRAY PROCESSING TECHNIQUES

Prepared by

Thomas W. Rekieta

Stanley J. Laster, Project Scientist
Frank H. Binder, Program Manager
Area Code 214, 238-6521

TEXAS INSTRUMENTS INCORPORATED
Services Group
P.O. Box 5621
Dallas, Texas 75222

Contract No. F33657-70-C-0100
Amount of Contract: $339,052
Beginning 15 July 1969
Ending 14 July 1970

Prepared for

AIR FORCE TECHNICAL APPLICATIONS CENTER
Washington, D. C. 20333

Sponsored by

ADVANCED RESEARCH PROJECTS AGENCY
Nuclear Monitoring Research Office
ARPA Order No. 624
ARPA Program Code No. 9F10

22 July 1970

Acknowledgment: This research was supported by the Advanced Research Projects Agency, Nuclear Monitoring Research Office, under Project VELA-UNIFORM, and accomplished under the technical direction of the Air Force Technical Applications Center under Contract No. F33657-70-C-0100.

AFTAC Project No. VELA/T/0701/B/ASD

NOISE STUDY FOR TFO EXTENDED SHORT-PERIOD ARRAY

Technical Report No. 5

SEISMIC ARRAY PROCESSING TECHNIQUES

Prepared by

Thomas W. Rekieta

Stanley J. Laster, Project Scientist
Frank H. Binder, Program Manager
Area Code 214, 238-6521

TEXAS INSTRUMENTS INCORPORATED
Services Group
P.O. Box 5621
Dallas, Texas 75222

Contract No. F33657-70-C-0100
Amount of Contract: $339,052
Beginning 15 July 1969
Ending 14 July 1970

Prepared for

AIR FORCE TECHNICAL APPLICATIONS CENTER
Washington, D. C. 20333

Sponsored by

ADVANCED RESEARCH PROJECTS AGENCY
Nuclear Monitoring Research Office
ARPA Order No. 624
ARPA Program Code No. 9F10

22 July 1970

Acknowledgment: This research was supported by the Advanced Research Projects Agency, Nuclear Monitoring Research Office, under Project VELA-UNIFORM, and accomplished under the technical direction of the Air Force Technical Applications Center under Contract No. F33657-70-C-0100.

This document is subject to special export controls and each transmittal to foreign governments or foreign nationals may be made only with prior approval of Chief, AFTAC.

Qualified users may request copies of this document from:

Defense Documentation Center
Cameron Station
Alexandria, Virginia 22314

TABLE OF CONTENTS

LIST OF ILLUSTRATIONS

LIST OF ILLUSTRATIONS (CONT'D)

ABSTRACT

Seismic data was digitally collected from the recently extended short-period array of the Tonto Forest Observatory during the summer of 1968 and the winter of 1969. An analysis of the data was made to characterize the ambient noise field from each period and to determine time- and space-stationarity of the fields. The effectiveness of multi-channel filter processing on the extended array was also measured.

Several contributors to the ambient noise field could be defined in both of the periods analyzed and appeared to be both time- and space-stationary. Other contributors, due primarily to atmospheric storm or pressure activity, were not stationary and could be related to its generating source.

Multi-channel filtering of the extended array could not provide any significant improvement over simple beamsteering at frequencies of interest (greater than .8 Hz). At lower frequencies, the amount of improvement obtained by MCF processing relative to beamsteering was directly related to the increase in noise level due to the non-stationary contributor of the noise field.

SECTION I
INTRODUCTION

Two data collection efforts were conducted at TFO for the purpose of recording high quality digital data from the recently extended short-period array and the three component long-period array. The data collected were classified as 'summer' data, consisting of the data collected during the period of 6 June to 21 June 1968, and as 'winter' data, which was recorded during the period of 27 January to 4 March 1969.

This report covers the TFO extended short-period array noise study. The primary objectives of the task were to compare the 'summer' and 'winter' noise field characteristics, to estimate the time and spacial stationarity of these noise fields, and to establish the effectiveness of multichannel processing using the extended array.

The analysis of the ambient noise field and the effectiveness of multichannel processing on the array outputs was conducted almost exclusively in the frequency domain using crosspower matrices developed from noise samples selected from each of the recording periods. A summary of the analysis and conclusion are presented in the next section. A detailed description of the processing and analysis of the data is presented in following sections.

BLANK PAGE

SECTION II

SUMMARY AND CONCLUSIONS

The ambient noise field of the extended short-period array at TFO was characterized from a spectral analysis of data samples selected from each of the recording periods. The time- and space-stationary of the coherent noise energy was measured from absolute single channel power-density spectra and from high resolution wavenumber spectra. The effectiveness of multichannel processing on the extended array was determined from the design and evaluation of MCFs on crosspower matrices of data from each of the periods being analyzed.

A. ANALYSIS OF THE AMBIENT NOISE FIELD

Absolute level of the ambient noise field was determined from single-channel power density spectra, computed by the Markov* technique. Significant changes in the absolute level of the power frequency energy were evident. The 'winter' samples showed a general increase in the absolute power level especially at frequencies below .25 Hz. The increases in the absolute levels of the power spectra appeared to be directly related to the amount and intensity of atmospheric pressure activity observed from weather maps. A significant increase in energy is observed in the area of .12 Hz during a 'winter' period of very intense atmospheric disturbance off the Alaskan Coast.

The spacial organization of the coherent noise energy during the winter and summer period was determined from high resolution frequency-wavenumber spectra computed for each of the periods.

Surface mode energy from the Northeast is observed during both periods. This energy is observed with the fundamental surface mode velocity of approximately 3.2 km/second at frequencies below .25 Hz. At higher frequencies this energy appears to travel at a higher velocity of approximately 3.6 km/second indicating the existence of higher-order surface mode energy.

---

* Burg, J.P., "Maximum Entropy Spectral Analysis" Society of Exploration Geophysicists

At frequencies of .4 Hz and greater the spacial organization of the coherent surface mode energy becomes isotropic in nature. At these frequencies a significant amount of P-wave energy from the South, with very high apparent horizontal velocities (40 km/second or greater) are consistently observed. Secondary P-wave contributions from the Northeast and Northwest with slightly lower apparent horizontal velocities are also observed.

The most significant difference in the spacial organization of the summer and winter ambient noise is the addition of noise from the Northwest as observed in the winter noise sample. At .12 Hz, the surface mode energy from this direction dominates the spectra. However, as the frequencies increase, the surface mode energy contribution from this direction rapidly decreases. The P-wave energy from the Northwest continues to be a significant contributor to the noise field up to frequencies of approximately .5 Hz. Analysis of the measured apparent horizontal velocity of the P-wave energy from the Northwest indicates the Alaskan storm to be the generating source.

A slight increase in the surface mode energy from the South and Southwest is also observed in the 'winter' data. In general the increase in the surface mode energy relates very well to the pressure activity in the corresponding direction.

High-resolution K-line spectra were computed to determine the relative contribution of each noise source to the total ambient noise power. The percent contributed as P-wave, directional surface mode, and isotropic surface mode is illustrated in Figure IV-18.

Based on the spectral analysis of the noise from the two time periods, the spatial organization of certain components of the coherent noise field, surface-mode energy from the Northeast and P-wave from the South, are stationary. However, the other surface-mode and P-wave components, which are highly influenced by seasonal and daily atmospheric variations or distrubances, are not time or space stationary.

B. ANALYSIS OF MCF PERFORMANCE

A set of multichannel filters were designed from a crosspower matrix computed from a long noise sample from each of the time periods. The signal-to-noise improvement was determined from a frequency domain application of the MCF to the noise and signal crosspower matrices used in the design. Results were compared to a similar applicaton of a simple beamsteer (straight summation) process to the same matrices.

Using 34 elements of the extend short-period array a S/N improvement of 23 db was obtained by MCF processing at the frequency of .12 Hz on the 'winter' data. Wavenumber analysis of MCF response shows this to be due primarily to the rejection of the surface-mode energy from the Northwest.

In general, some S/N improvement can be obtained by MCF processing over that of beamsteering at frequencies below .75 Hz. On the 'summer' data, S/N improvements of 3 to 6 db above that of the beamsteering processing was obtained by MCF processing. Additional gain is obtained on noise samples which have an increase in coherent energy at these frequencies due to the previously discussed atmospheric activity. However, since the generating source is not considered as space stationary, on line processing with fixed MCFs is not expected to provide any significant improvement. At frequencies above .8 Hz, MCF processing of the extended array would not provide any significant signal-to-noise improvement over beamsteering even under stationary conditions.

SECTION III

PREPARATION OF DATA FOR ANALYSIS

Large quantities of seismic data were collected from the extended short-period array on a Digital Field System (DFS) operated by Texas Instruments' engineers during two recording efforts. The first recording session covered the period of 6 June 1968 to 21 June 1968. Data from this period will be designed as 'summer' data. The second recording period, during which 'winter' data were recorded covered the period from 27 January 1969 to 3 March 1969. This section outlines the pre-processing performed on noise samples selected from the recorded data for extensive analysis. For reference, Figure III-1 shows the relative locations of the extended short-period array elements from which the data was collected.

A. EDITING OF DATA

The 'summer' data was recorded during a period when severe spiking problems on array elements were being experienced on the recently extended array. Several segments of the data, covering approximately two hours, were selected and edited from the field tapes. One of these samples recorded on 19 June 1968, containing 33 channels of seismic data (elements Z32, Z6, Z18, and Z20 were inoperative) was then processed with a program to detect and remove the undesired spikes from the data.

The data was recorded by the DFS with a sampling interval of .096 seconds. Since the noise energy at the higher frequencies (greater than 1.5 Hz) was expected to be random across the extended array due to the large interelement spacing, the data was high-cut (anti-aliased) filtered and resampled to provide a sampling interval of .288 seconds and a frequency band of 0 - 1.736 Hz. The data was also pre-whitened as shown by Figure III-2.

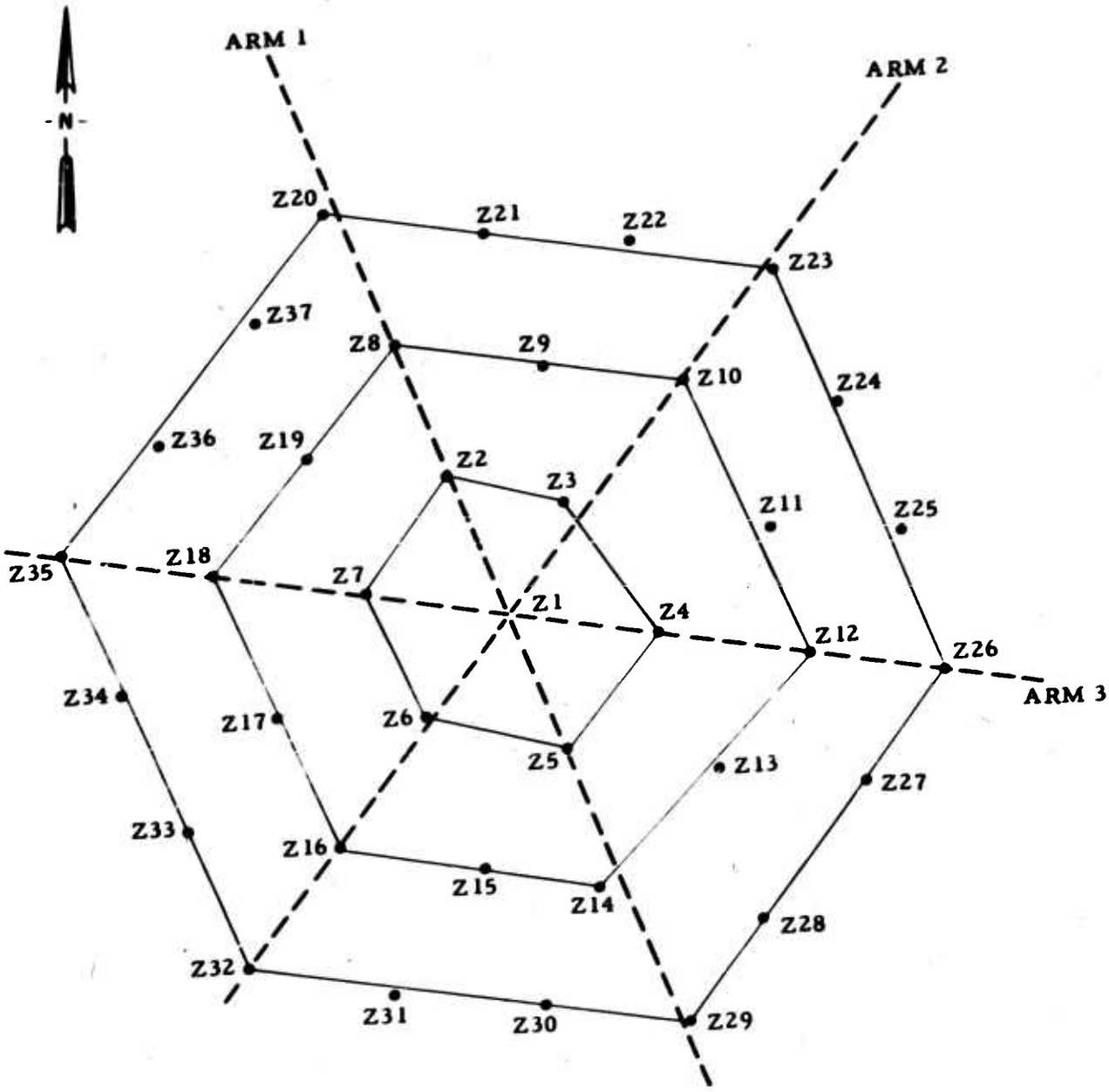

Figure III-1. Extended Short-Period Array at TFO

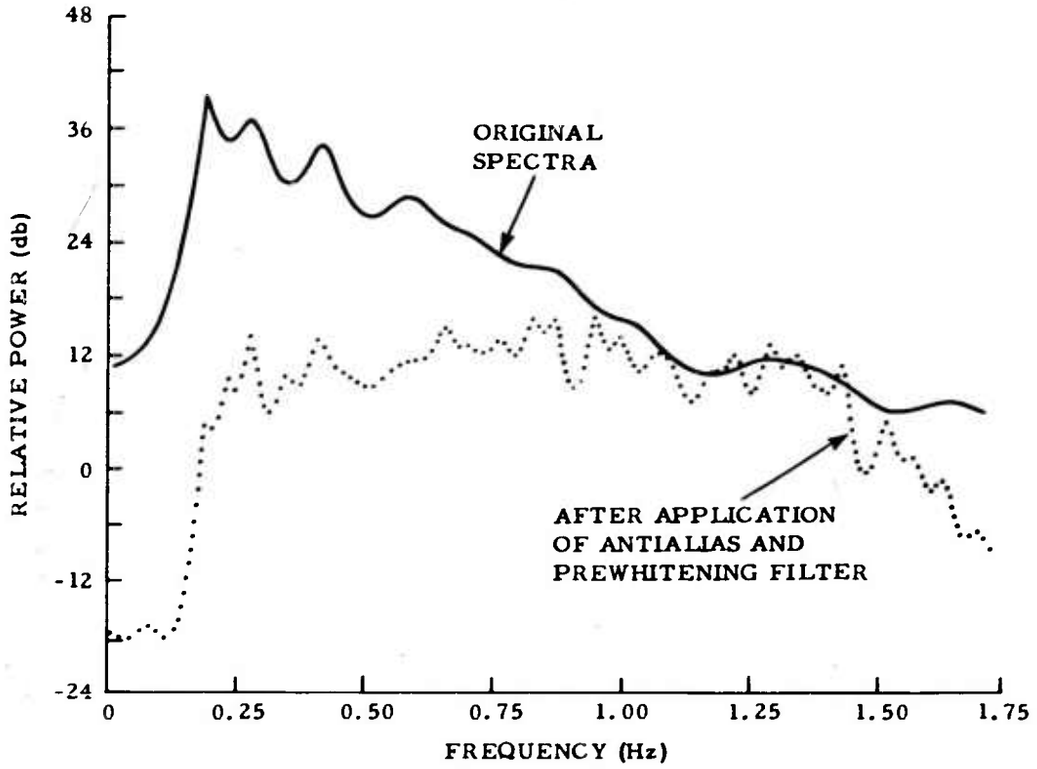

Figure III-2. Spectra Illustrating Effects of Anti-Alias and Pre-Whitening Filter.

Similarly, several segments of data were edited from the 'winter' data tapes. One of the noise samples recorded on 27 february 1969 during which intense low pressure conditions were observed from weather maps, was selected for a detailed analysis. However, due to bad spots in the data such as missing elements and severe spiking,only 50 minutes of data from any recording was acceptable for analysis. All but three (Z19, Z22, and Z31) of the 37 array elements were operating satisfactorily. The data was anti-aliased filtered and resampled to provide the .288 second sampling interval.

B. DEVELOPMENT OF X-POWER MATRICES

The fast Cooley-Turkey transform method was used to obtain the frequency domain representation of the 'summer' and 'winter' noise samples. The crosspower matrices were developed for each of the noise samples as follows.

1. 'Summer' Data

The time traces of the 'summer' data was transformed using gates of 512 points of data at a time. A total of 45 gates were transformed. Crosspower matrices for the 33 channels of data were computed from the transforms for each of the 257 frequencies covering the band 0.0 to 1.736 Hz in .00678 Hz increments. The matrices were then stacked for all the transform gates and smoothed across frequencies by an equal weighting function for five adjacent frequencies. Every fifth frequency was saved for further analysis resulting in a set of 51 matrices for the 0-1.736 Hz band at a frequency increment of .0339 Hz between matrices. The spectral window due to the transform gate and smoothing described is shown in Figure III-3.

2. 'Winter' Data

The 'winter' time traces were transformed in 256 point segments resulting in 129 complex frequency values for the 0 to 1.736 Hz frequency band. A total of 40 segments were transformed for the 34 channels of data. Crosspower matrices were computed from the transforms and stacked. In this case, smoothing of the matrices was performed across three adjacent frequencies with equal weighting of matrices. This resulted in a set of 43 matrices covering the frequency band of the data in .041333 Hz increments. The effective spectral window for this data is also shown in Figure III-3.

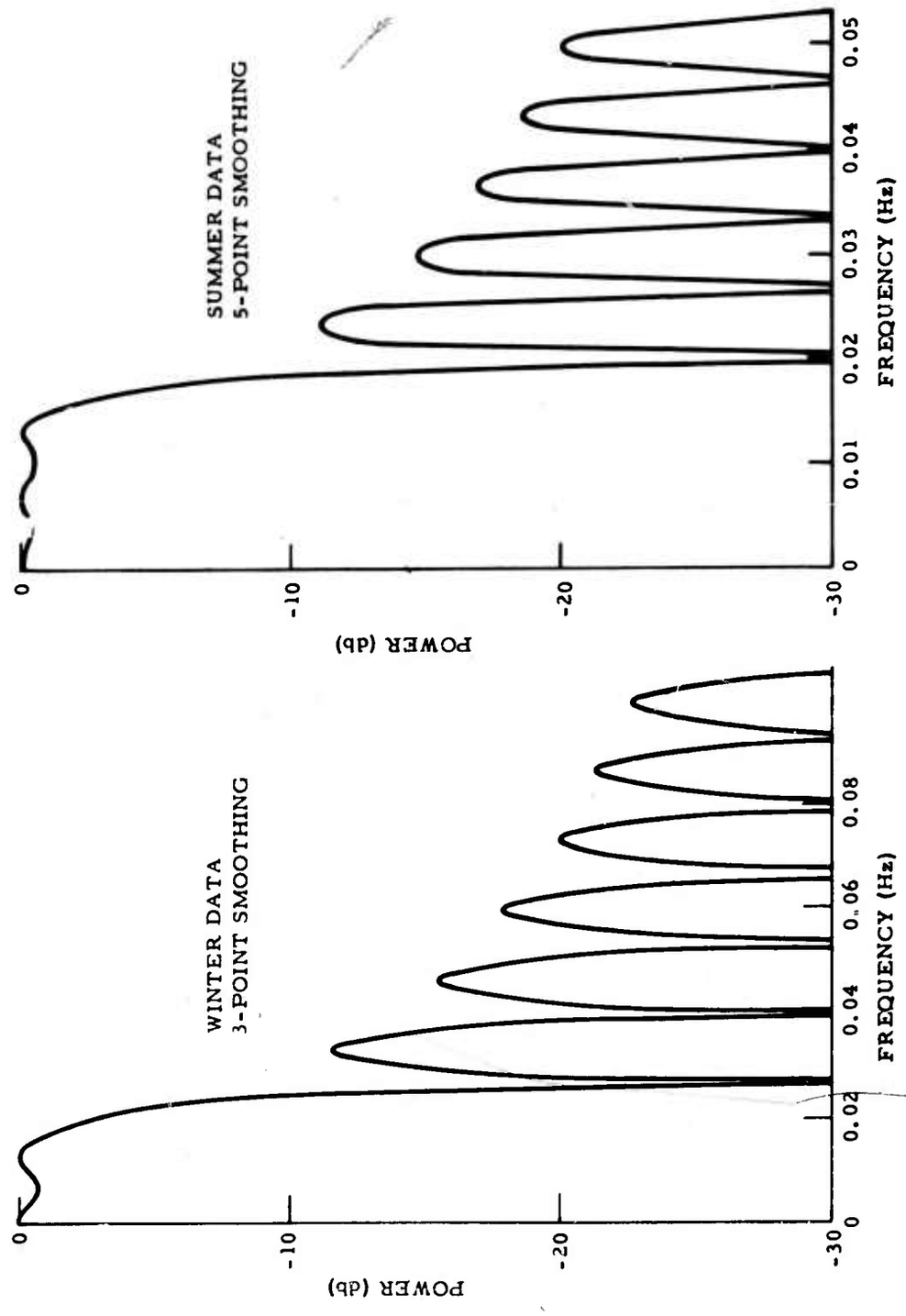

Figure III-3. Spectra Window of the Crosspower Matrix Computed from the TFO Noise Samples

SECTION IV

ANALYSIS OF AMBIENT NOISE FIELDS

The characteristics of the 'winter' and 'summer' noise field were determined and compared through an analysis of single channel-power density spectra, frequency-wavenumber spectra and $\vec{K}$-line spectra for the extended short-period array. The time- and space-stationarity of the noise field were estimated from the noise samples analyzed.

A. SINGLE-CHANNEL POWER-DENSITY ANALYSIS

Power density spectra were estimated, using the Markov Spectral Estimation Technique for several channels from each of the noise samples studied.

The daily 1.0 Hz calibration of the array sensors were recorded by the DFS and used in this study to establish absolute levels for the spectra. The resulting spectra for the 'winter' and 'summer' data are shown in Figures IV-1 and IV-2 respectively.

A comparison of the spectra show an increase of approximately 6 db in noise power for the 'winter' sample across all frequencies shown. A larger power increase of approximately 12 db is observed in the area of .25 Hz.

During the period which the 'winter' data was recorded, intense lows occurred at several locations along the coast lines. The strongest of these were situated off the west coast of Alaska. Others existed along the west coast of continental U.S., west coast of Mexico, Gulf of Mexico, in the Baffin Bay, east coast of Greenland, and along the eastern coast line of U.S. near the New England states. The 'summer' sample used in the analysis was recorded during a period of relative little storm activity. However, another 'summer' noise sample was selected for the single-channel spectral analysis, which was recorded

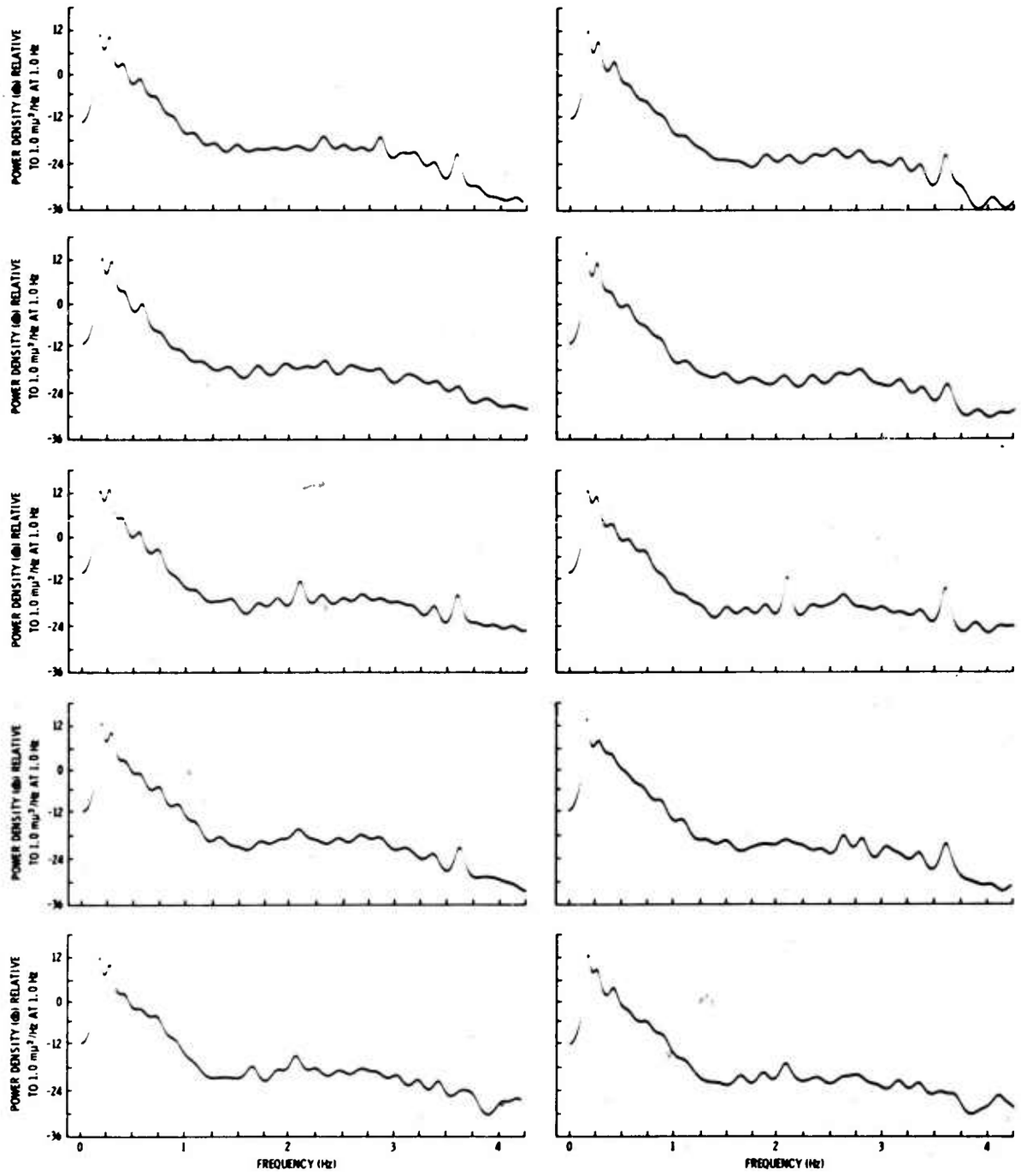

Figure IV-1. Single-Channel Power Density Spectra From 'winter' Recording Period

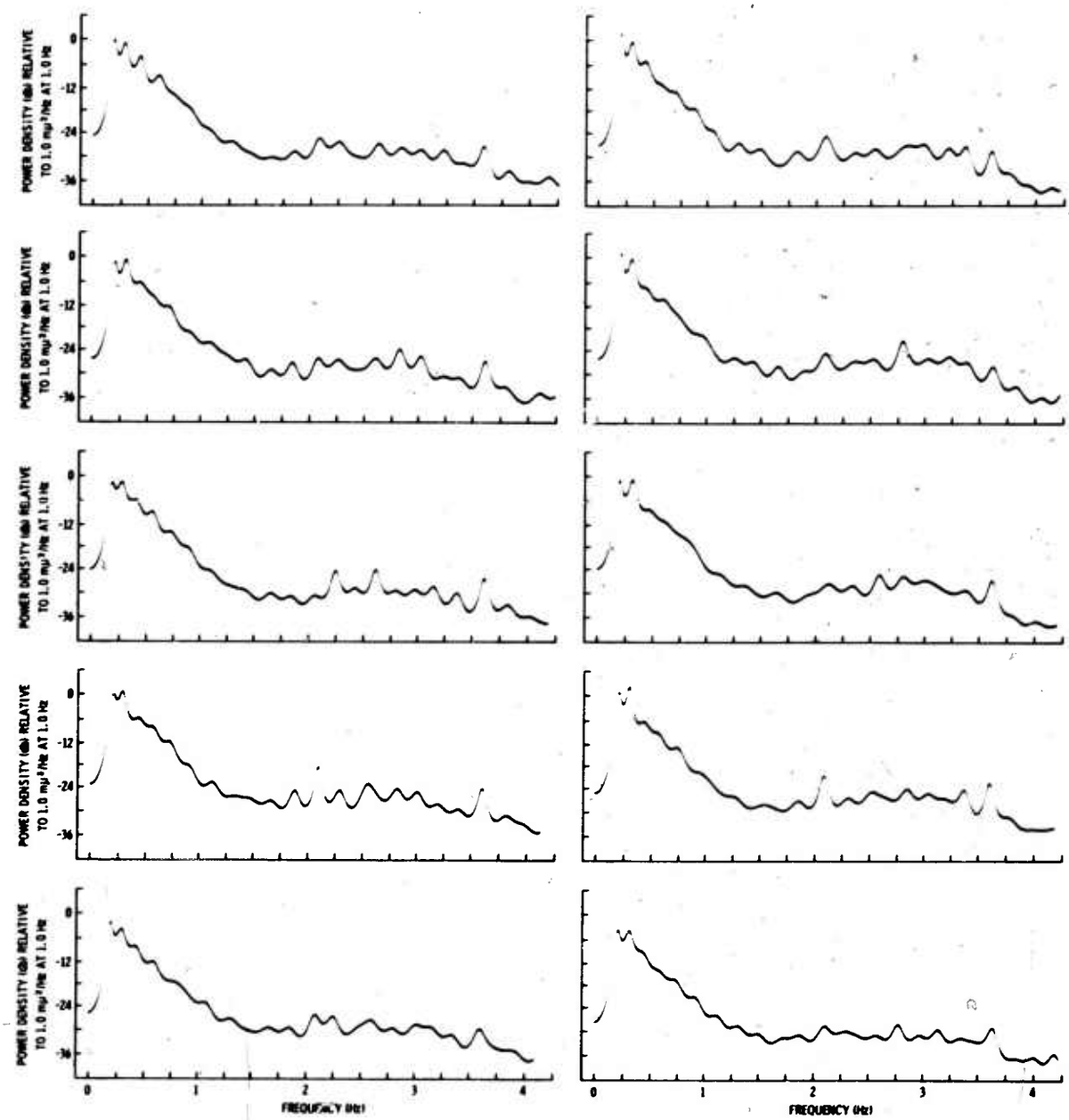

Figure IV-2. Single-Channel Power Density Spectra From 'summer' Recording Period

during a period when some intense atmospheric activity was occurring off the Newfoundland coast. This sample 10 June, will be classified as 'noisy summer' data. A comparison of the spectra from the 'winter' and two 'summer' data samples is presented in Figure IV-3. The 'noisy summer' sample, has a comparable noise level to the 'winter' data in the .3 to 1.0 Hz frequency band. It does not show the large increase in noise energy below .3 Hz as observed in the 'winter' data. The following wavenumber analysis will show this increase in energy below .3 Hz in the 'winter' noise to be due primarily to the intense low pressure activity off the Alaskan coast.

B. HIGH-RESOLUTION FREQUENCY WAVENUMBER ANALYSIS

The crosspower matrices, Φ, developed in Section III for each of the noise samples were used to compute high-resolution wavenumber spectra at frequencies in the .12 to .6 Hz band. Spectra from higher frequencies become difficult to interprete due to the spacial alaising of the array. The method used to compute the spectra is described by:

$$P(\bar{k})^2 = \frac{1}{\sum_{i=1}^{NC} V^H \Phi^{-1} \Gamma_i \Gamma_i^H \Phi^{-1} V} = \frac{1}{a^2 V^H \Phi^{-2} V}$$

where

NC = number of array sensors,

V is the column vector

$$\begin{bmatrix} e^{i2\pi \bar{k} \cdot X_1} \\ e^{i2\pi \bar{k} \cdot X_2} \\ \vdots \\ e^{i2\pi \bar{k} \cdot X_{NC}} \end{bmatrix}$$

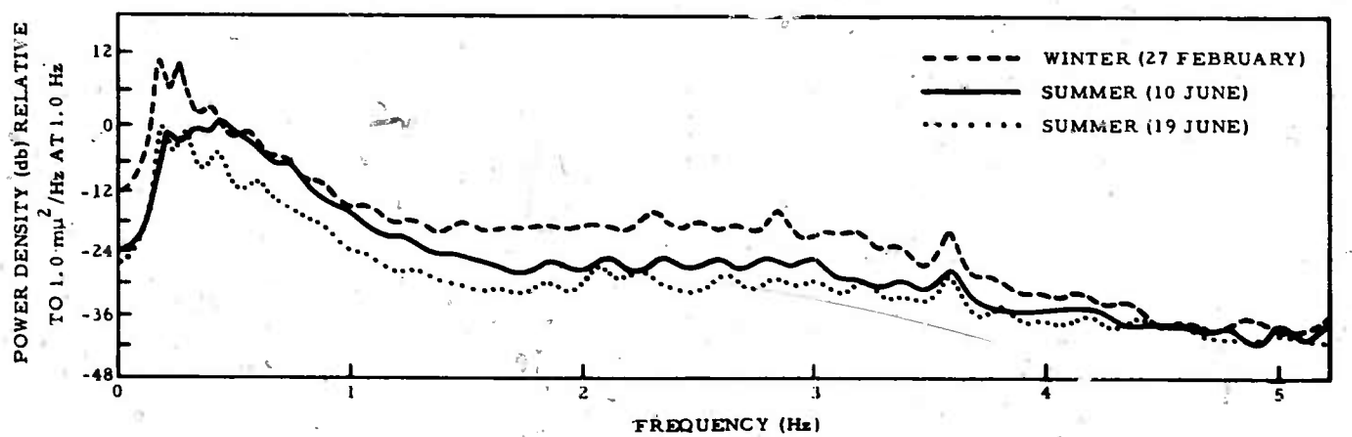

Figure IV-3. Comparison of 'winter' and 'summer' Single-Channel Power Density Spectra.

and Γ_i is the reference vector for the i^{th} sensor, i.e. all components are zero except the one corresponding to the sensor being referenced.

$$\Gamma_2 = \begin{bmatrix} 0 \\ \alpha \\ 0 \\ \cdot \\ \cdot \\ \cdot \\ 0 \end{bmatrix}$$

where α is a positive non-zero value.

1. 'Summer' Surface-Mode Spectra

High-resolution wavenumber spectra computed at the frequencies of .169, .203, .236, .270, .304, .338, .372, and .405 Hz from the 'summer' noise matrices are shown in Figure IV-4 through IV-7. The edge velocity of each of the spectra is 2.0 km/second. A dashed circle is shown on the spectra to illustrate the approximate velocity of surface mode energy.

In the first figure, the surface mode energy from the Northwest appears to be a principal contributor to the noise field along with the P-wave energy from the South. Measurements of the surface mode peak indicates an apparent velocity across the array of 3.17 km/second. A secondary surface mode peak at approximately the same velocity is observed from the Southwest.

As the frequencies are increased the surface mode peaks rapidly decrease in relative power and the p-wave from the south becomes predominant. The surface mode energy becomes very isotropic in nature with a measured velocity of 3.2 km/second. There is continued evidence of directional surface mode energy from the Northeast at the higher frequencies, however, the apparent velocity is somewhat higher than that previously measured for the directional contribution and that of the isotropic noise indicating that it is traveling as some higher order mode energy.

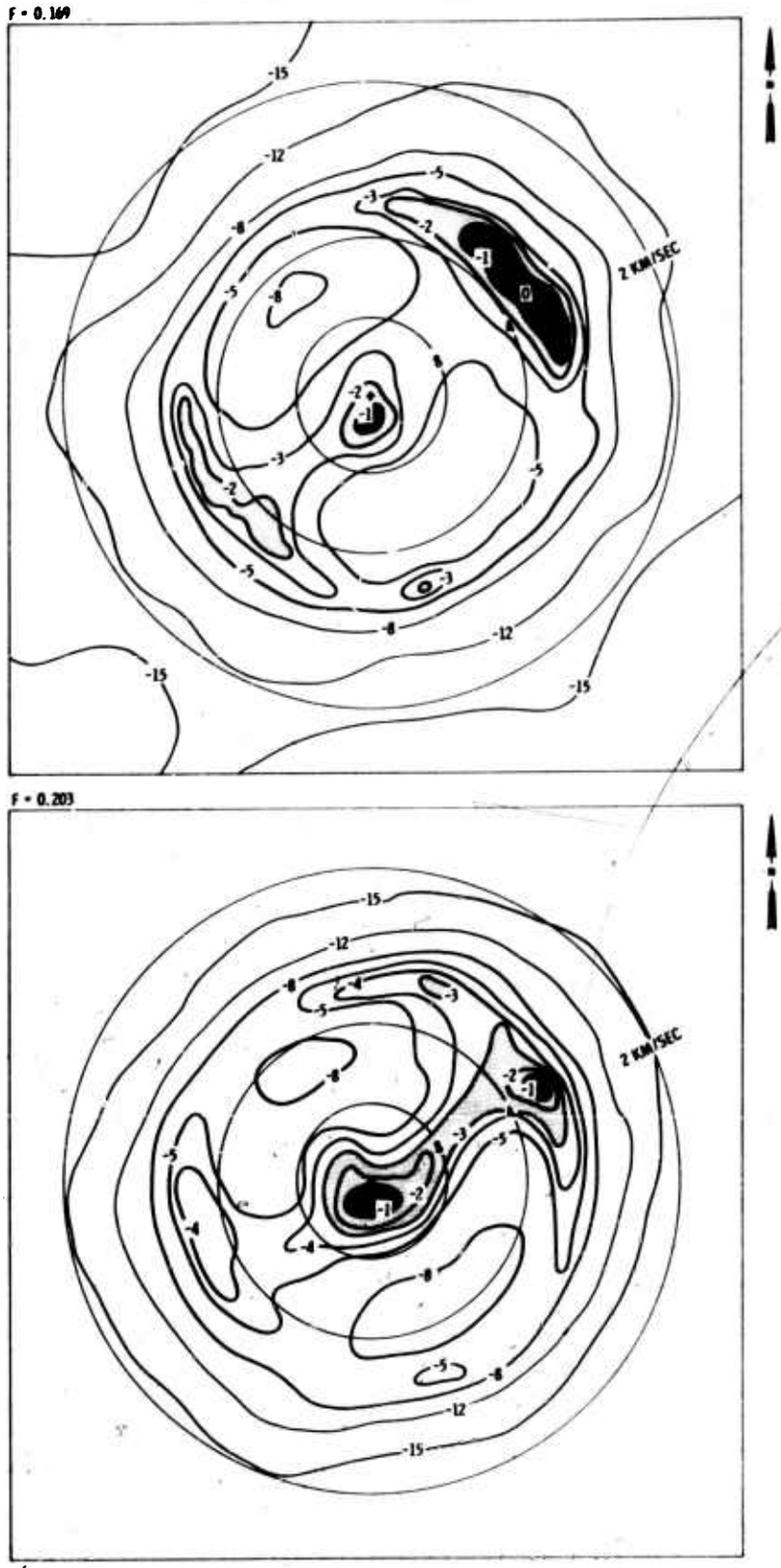

Figure IV-4. High Resolution Wavenumber Spectra of .169 and .203 Hz 'summer' Noise

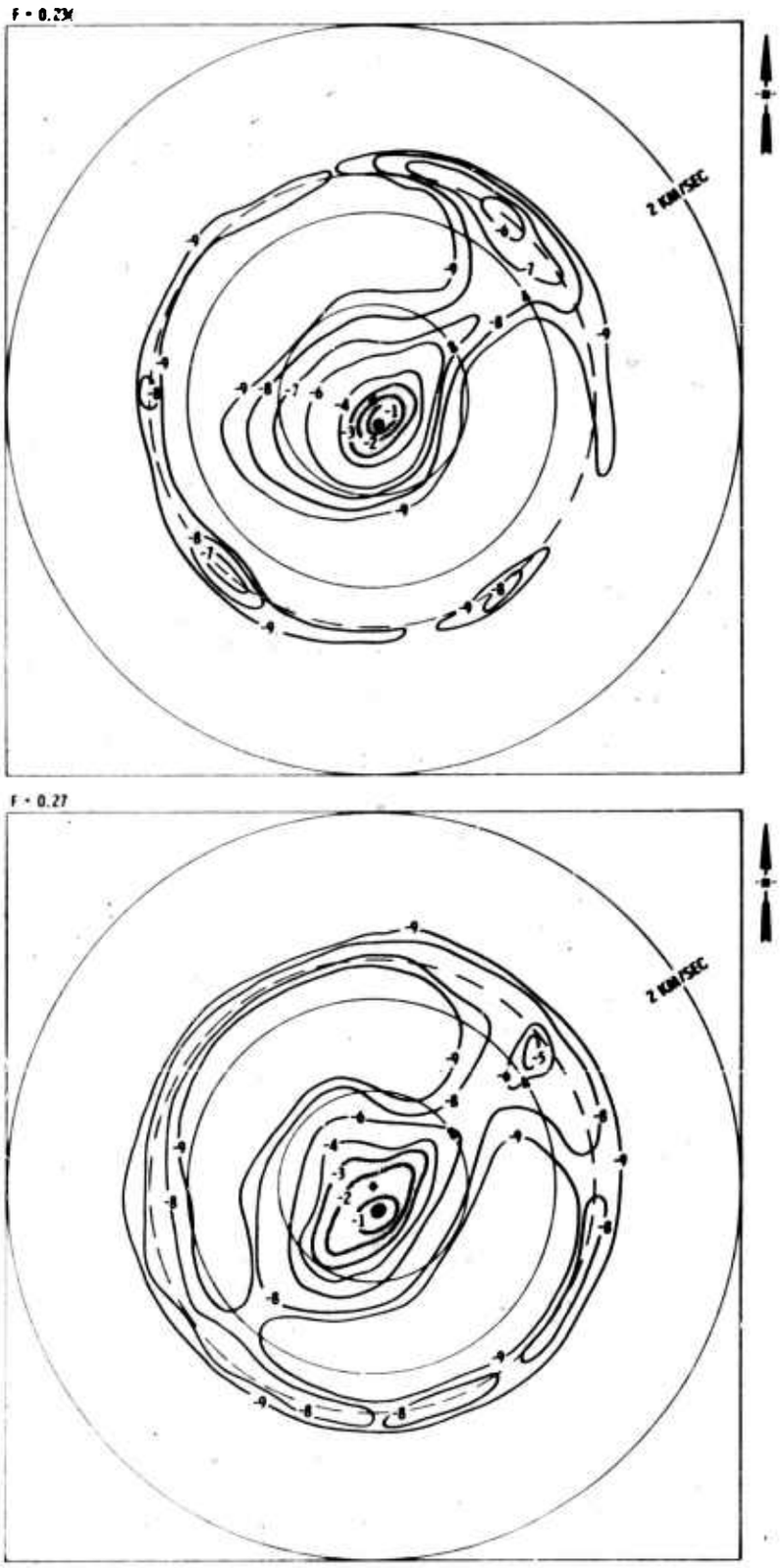

Figure IV-5. High Resolution Wavenumber Spectra of .23 and .27 Hz 'summer' Noise

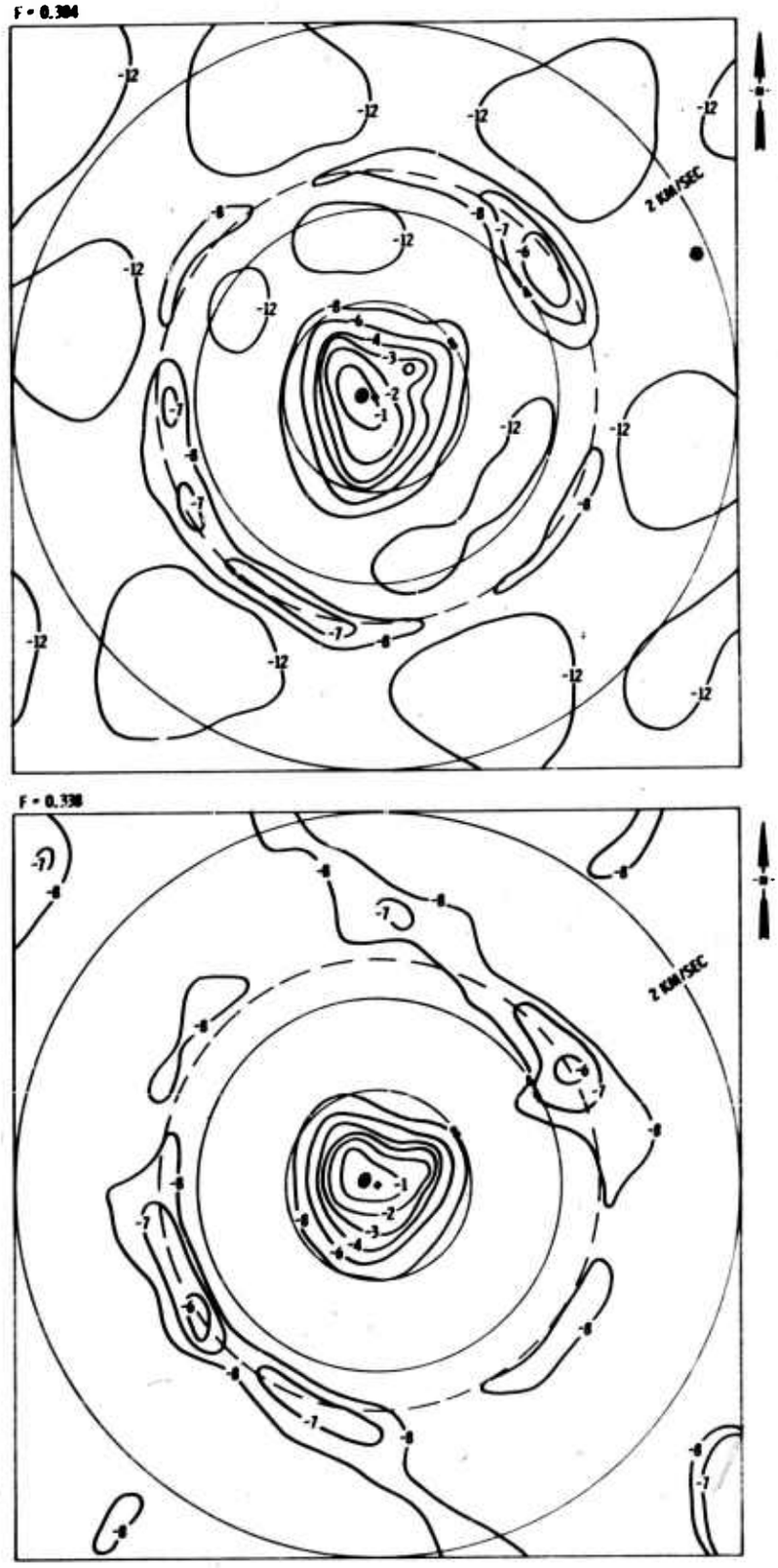

Figure IV-6. High Resolution Wavenumber Spectra of .304 and .338 Hz 'summer' Noise

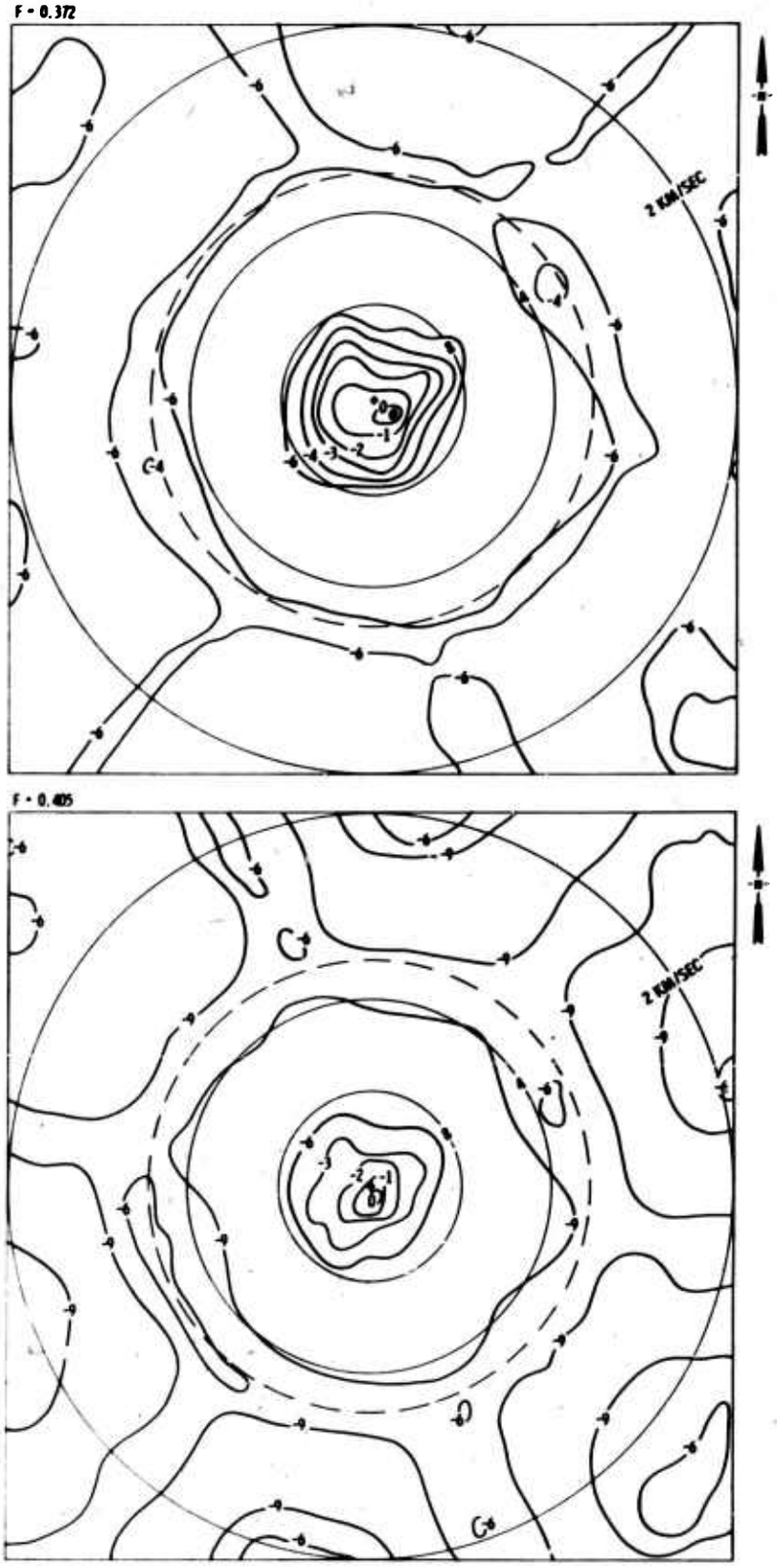

Figure IV-7. High Resolution Wavenumber Spectra of .372 and .405 Hz 'summer' Noise

The energy arriving from the Northeast is believed to be generated in the area of Newfoundland and the eastern coast of Canada and the US based on the spacial organization of P-wave energy and the correlation of atmospheric activity in this region to increased surface mode noise from this direction. The path of such surface mode noise would transverse the Rocky Mountain region which could possibly cause the higher order mode energy observed at the higher frequencies. That is the higher-mode excitation might have been effected by the fundamental mode impinging on the discontinuity of the mountainous range.

2. 'Summer' P-Wave Spectra

At the higher frequencies the resolution of the array becomes sufficient to show the P-wave noise field consists of several contributors. In an effort to analyze the P-wave noise in detail, wavenumber spectra with an edge velocity of 10.0 km/second were computed and are shown in Figures IV-8 and IV-9 for the frequencies of .507, .541, .574, and .608 Hz.

As observed in these spectra the principle p-wave contribution is from the south with an apparent horizontal velocity of 30 to 40 km/second. As the frequencies increase, the direction of this energy shifts slightly from east to west.

A contributor to the p-wave field is also shown in the same direction as the earlier observed surface mode energy from the Northeast. Weather maps of this period show low pressure activity near the southern tip of Greenland. Events occurring in this area would arrive at TFO with an azimuth of 31 degrees and an apparent horizontal velocity of 15.5 km/second. The average velocity and azimuth of the Northeast peak in Figure IV-9 is 15 km/second and 40 degrees, respectively, indicating generating source to be in general area of the atmospheric activity.

Similarly, the p-wave contribution from the Northwest can be related to low pressure activity below Alaska. The azimuth of the energy peak in the wavenumber spectra is measured to be approximately 315 degrees and the velocity range is 11.3 to 15.8 km/second. An event occurring off the Southern coast of Alaska in the area of the storm activity would arrive at TFO with an azimuth of 323 degrees and a velocity of 12.4 km/second.

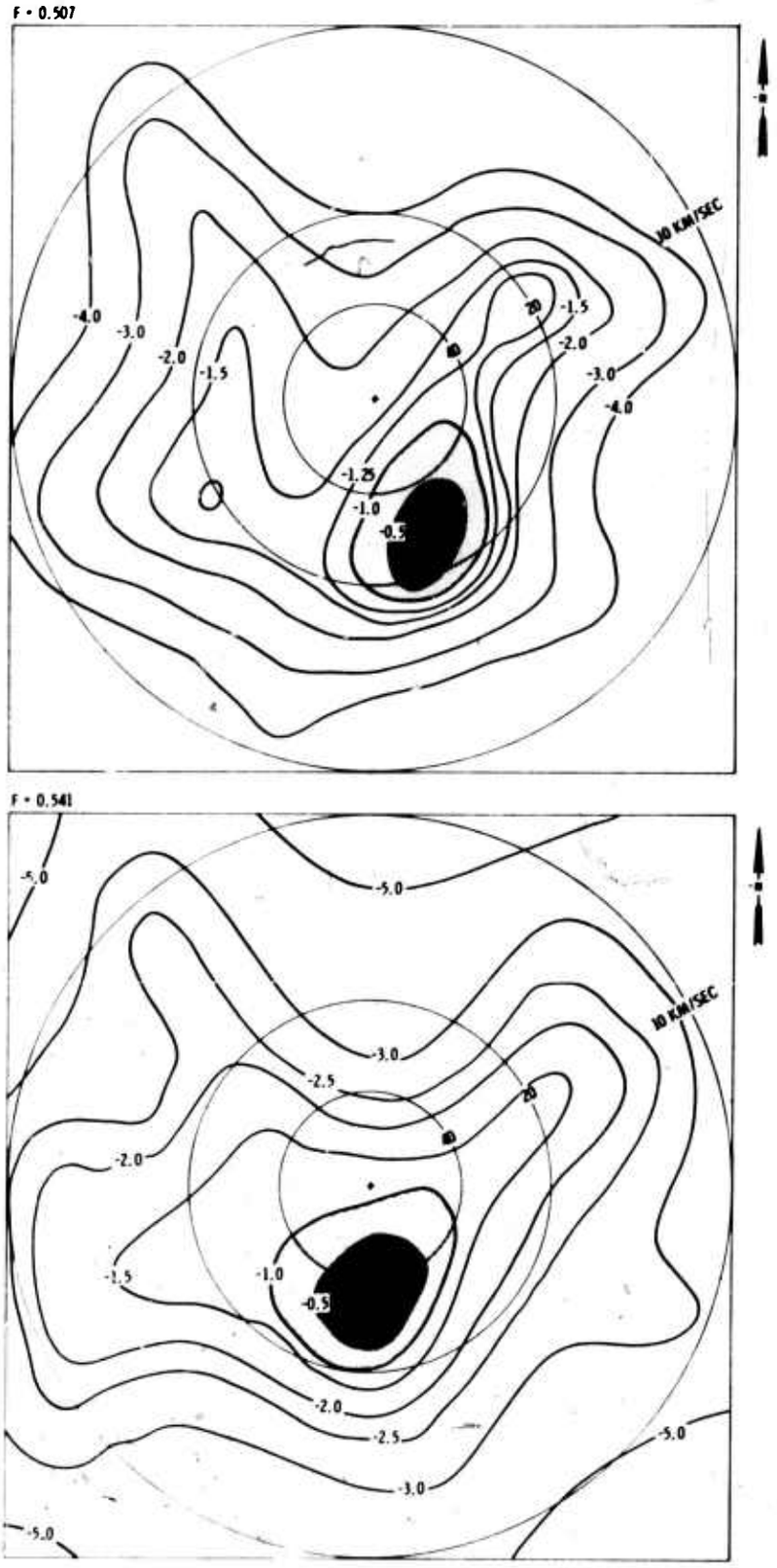

Figure IV-8. High Resolution Wavenumber Spectra of 'summer' P-Wave Noise at .507 and .541 Hz

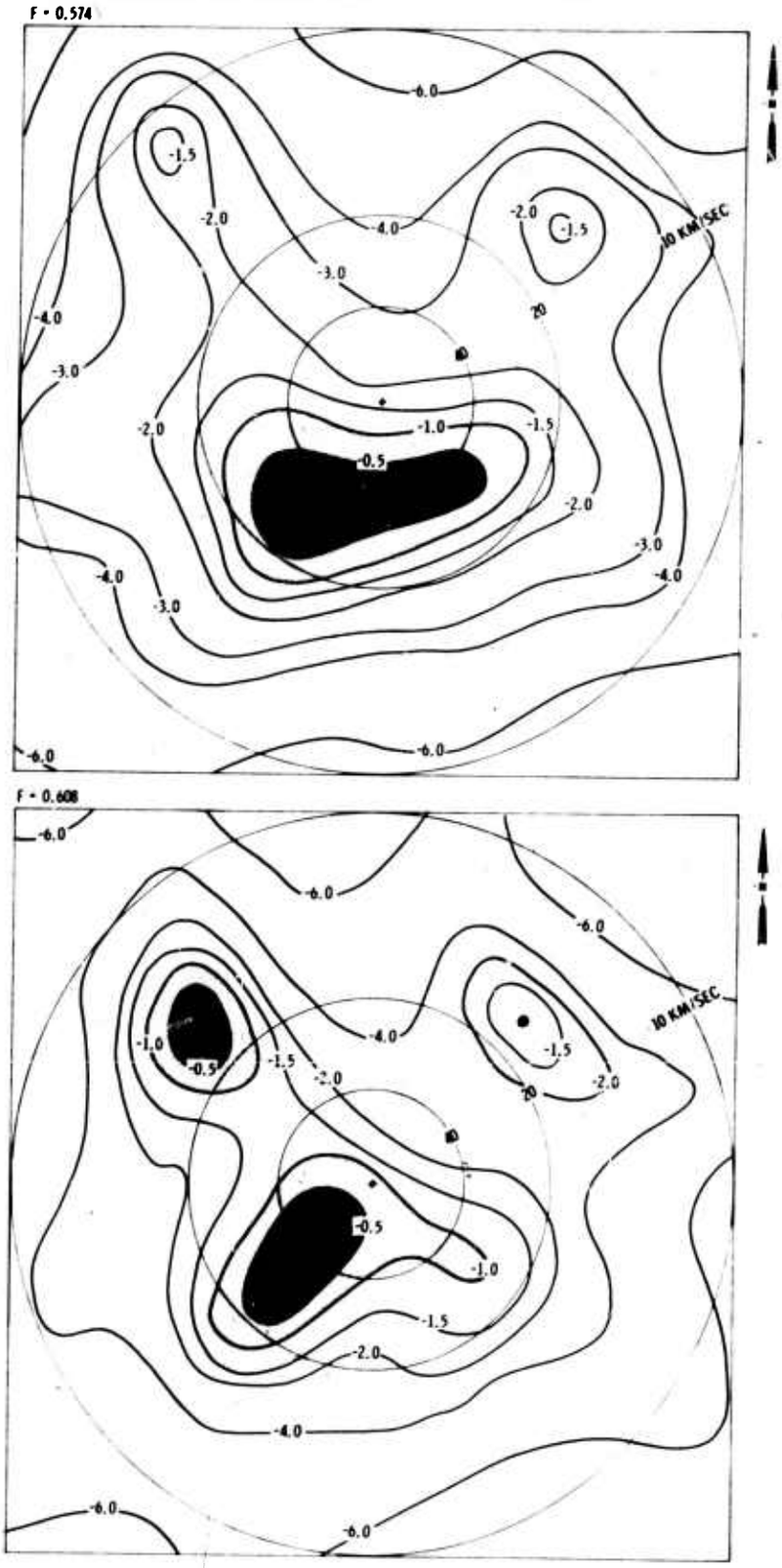

Figure IV-9. High Resolution Wavenumber Spectra of 'summer' P-Wave Noise at .574 and .608 Hz

3. 'Winter' Surface-Mode Spectra

Analysis of the single-channel power density spectra showed significant energy increase at very low frequencies in the 'winter' sample. A high resolution wavenumber spectra computed at the frequency of .12 Hz (Figure IV-10) indicates this increase resulted primarily from a strong surface-mode energy contribution from the Northwest in the direction of the previously mentioned intense low pressure disturbance off the Western coast of Alaska. However the high resolution technique also indicates a second peak in the spectra at this frequency is 180^{o} to the previous one and is at a somewhat lower velocity. An analysis of wavenumber spectra computed by conventional methods were compared to the high resolution spectra to establish authenticity for each of the observed energy lobes. Conventional spectra computed at .12 Hz gave no indication of noise energy from the direction of this second lobe. It is more likely due to effects resulting from the strong highly coherent noise source from the Northwest. Similar effects have been observed in wavenumber responses of MCF's designed using noise statistics consisting of a single highly coherent noise component. At the higher frequencies, the percentage of the total coherent noise energy contributed by a single source is significantly less than that observed for the Northwest component at .12 Hz, thereby restricting such effects.

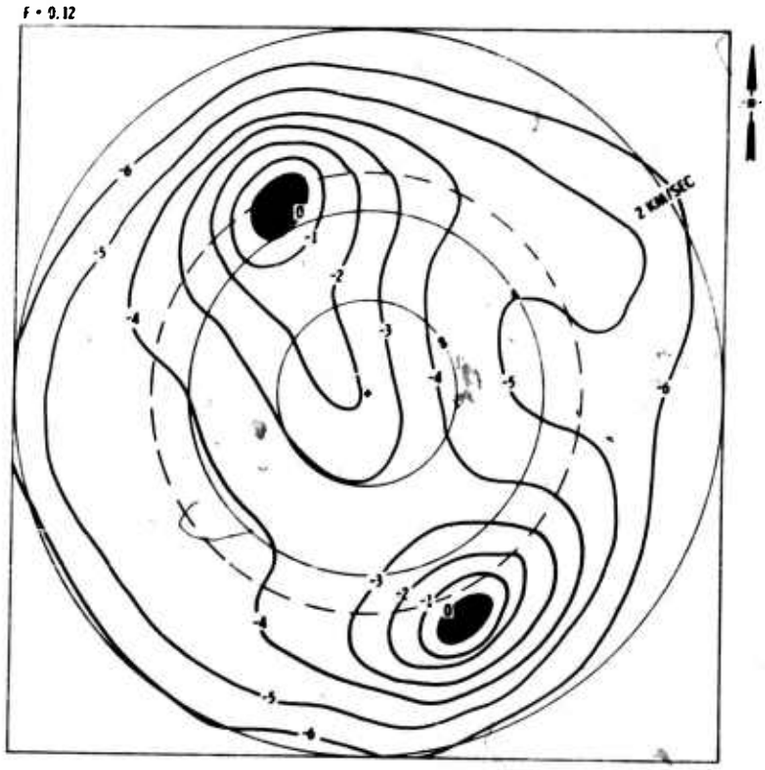

Figure IV-10. High Resolution Wavenumber Spectra of the .12 Hz 'winter' Noise

In Figure IV-11 the wavenumber spectra for the frequencies of .163 and .203 Hz are shown, in which additional surface mode lobes, similar to those observed in the 'summer' sample, are evident. The multiple surface mode lobes are in close agreement with expectations based on the numerous atmospheric disturbance observed from weather maps.

At the higher frequencies of .24 to .41 Hz (Figures IV-12 and IV-13), the generating source to the Northeast of the array becomes the principle contributor to the surface-mode energy as previously observed in the 'summer' data. However, the principle p-wave contributor for the 'winter' noise is from the Northwest (Alaskan activity) contrary to the predominant Southern P-wave contributor in the 'summer' data.

4. 'Winter' P-Wave Spectra

High resolution wavenumber spectra were computed with an edge velocity of 10 km/second at the higher frequencies of .41, .49, .57, and .61 Hz to determine the spacial structure of the 'winter' p-wave. These spectra are shown in Figure IV-14 and IV-15.

At .41 Hz the predominant contributor of p-wave is observed to be from the Northwest and a secondary contribution from the South. As the frequencies are increased the Southern contribution continually increases in relative energy contribution over that of the Northwest source.

The average velocity and azimuth of the p-wave energy from the Northwest was measured from the four spectra to be 15.3 km/second and 320 degrees. P-wave energy originating in the area of the atmospheric activity near the Western coast of Alaska would arrive at TFO with an apparent horizontal velocity of 13.9 km/second and an azimuth of 326 degrees.

As in the 'summer' data, the p-wave energy due to the Southern contribution has a very high apparent horizontal velocity of 40 km/second or higher. A possible generating source of the p-wave energy from the South could not be defined.

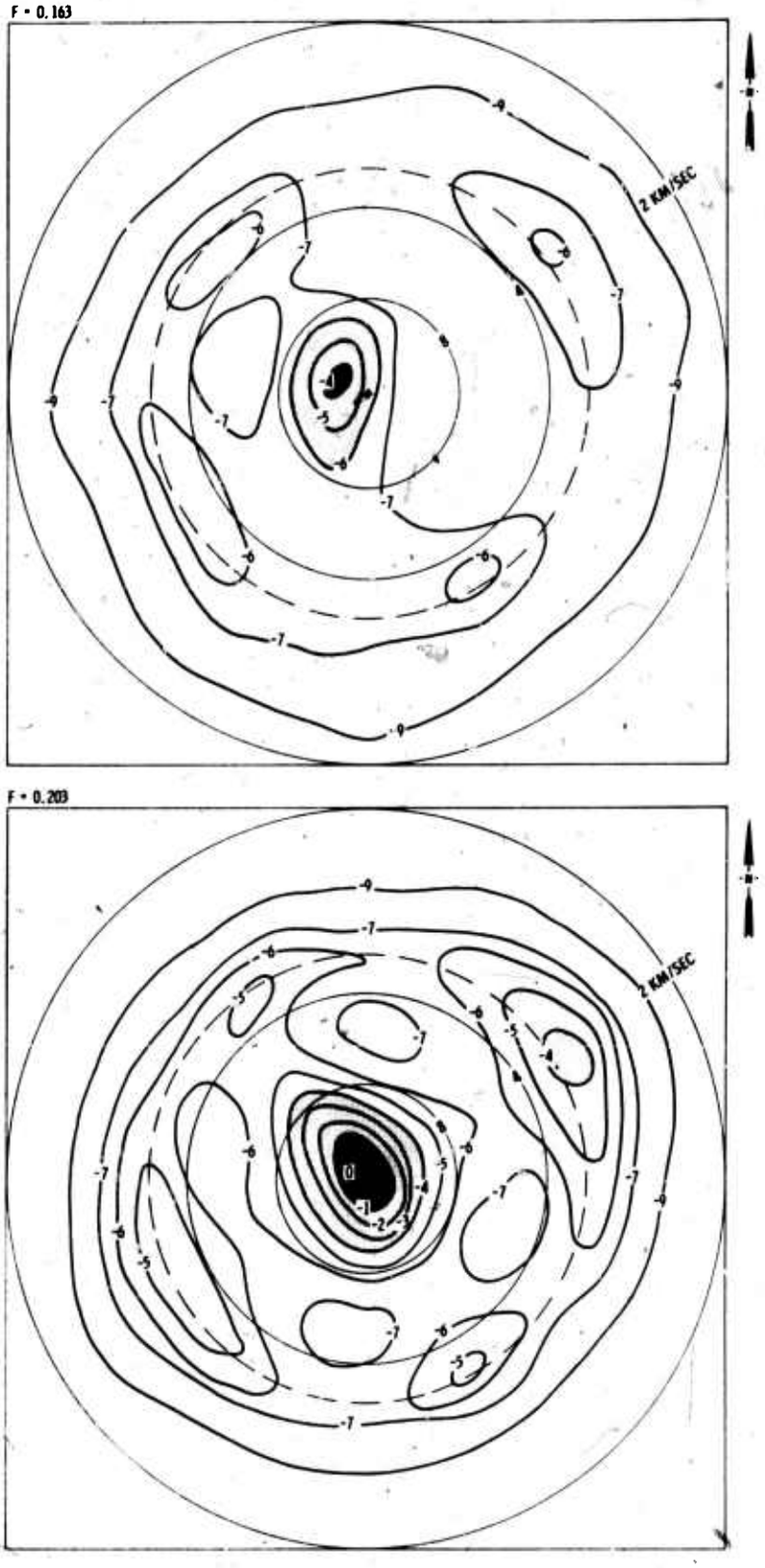

Figure IV-11. High Resolution Wavenumber Spectra of .163 and .203 Hz 'winter' Noise

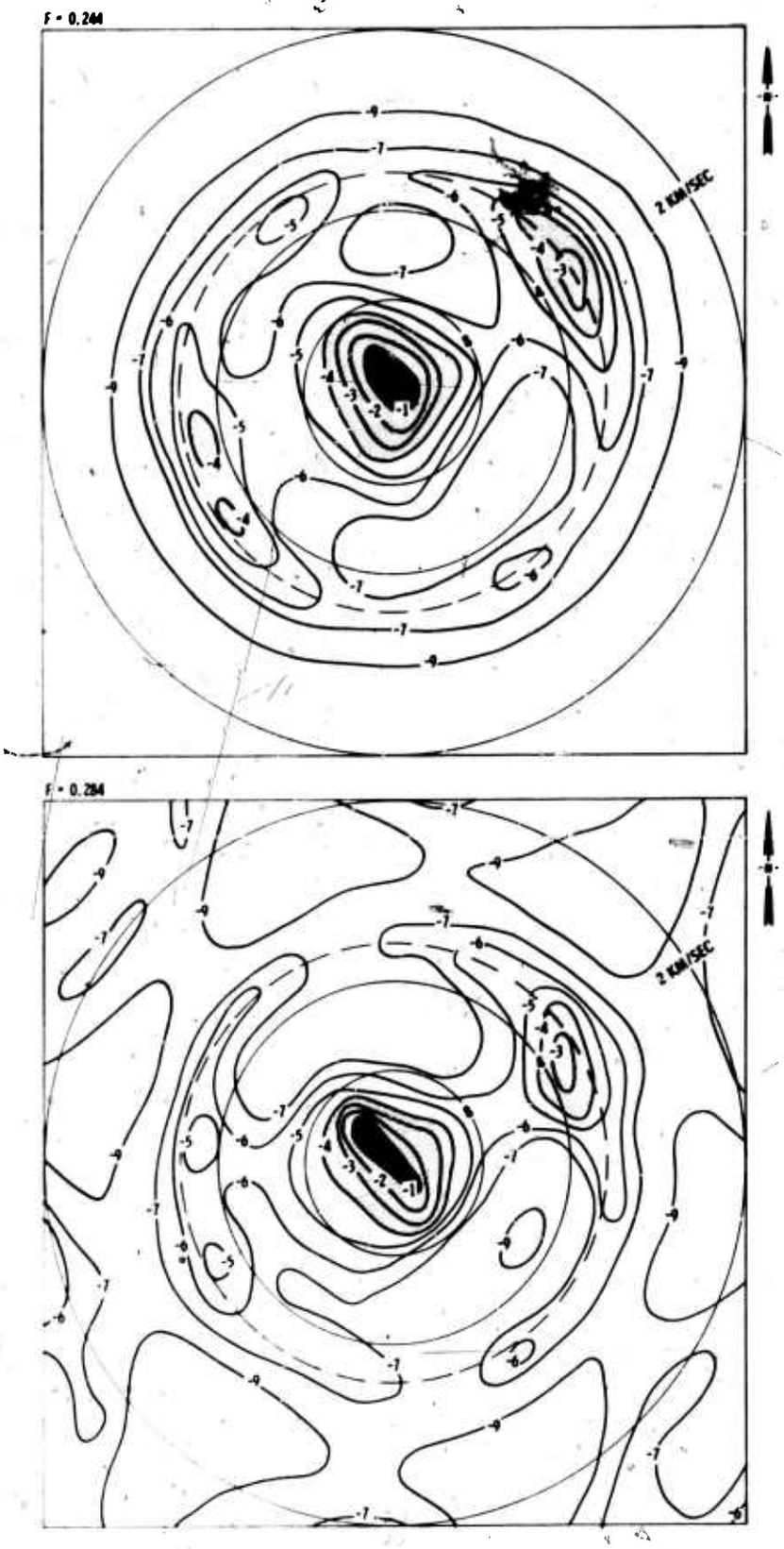

Figure IV-12. High Resolution Wavenumber Spectra of .244 and .284 Hz 'winter' Noise

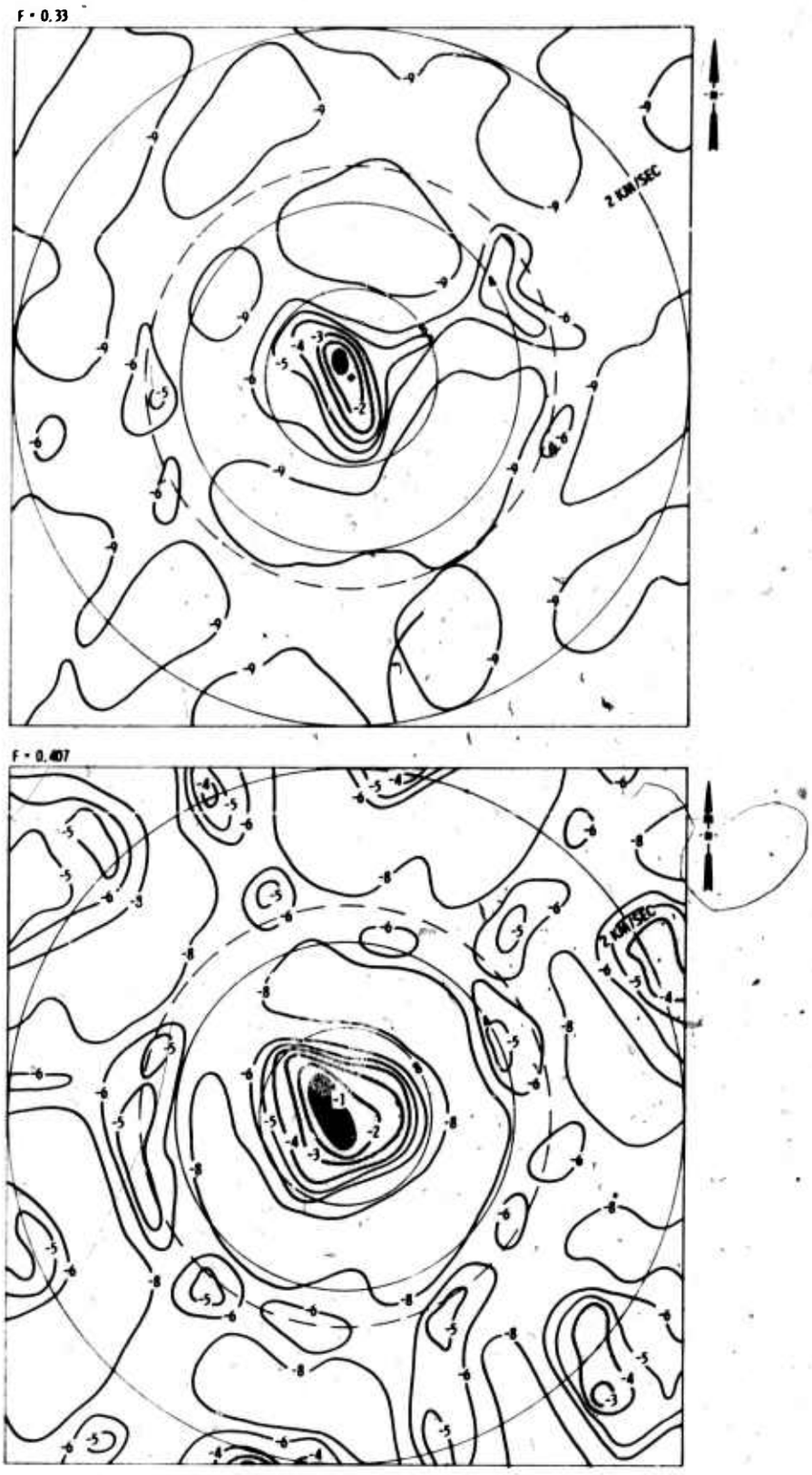

Figure IV-13. High Resolution Wavenumber Spectra of .33 and .407 Hz 'winter' Noise

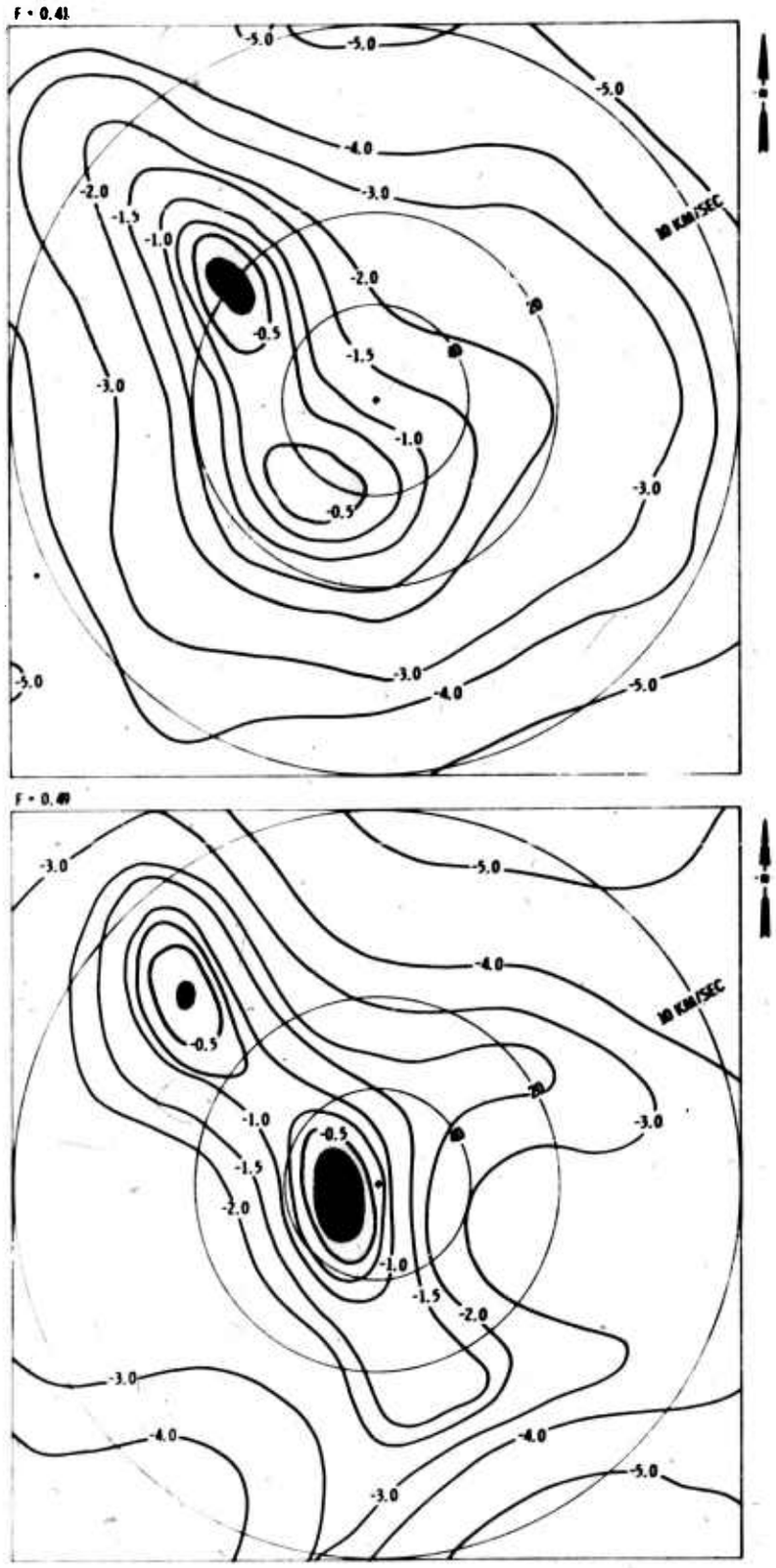

Figure IV-14. High Resolution Wavenumber Spectra of the 'winter' P-Wave Noise at Frequencies of .41 and .49 Hz

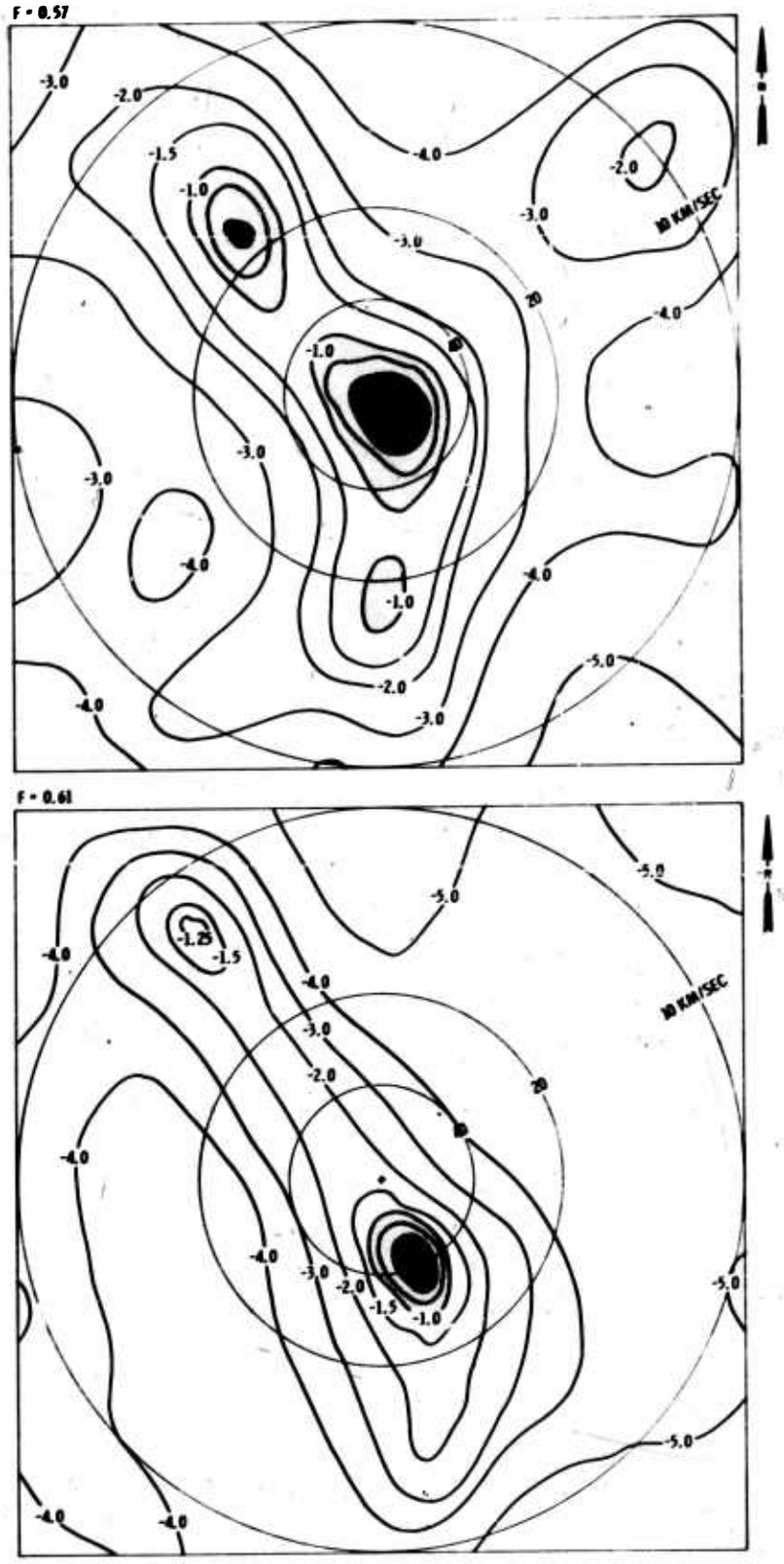

Figure IV-15. High Resolution Wavenumber Spectra of the 'winter' P-Wave Noise at Frequencies of .57 and .61 Hz

C. $\vec{K}$-LINE SPECTRAL ANALYSIS

The 1-dimensional wavenumber ($\vec{K}$-line) spectra presented and analyzed in this section can be interpreted as the physical projections of the 2-dimensional power density wavenumber spectra, similar to that discussed in previous subsection, onto axes which are parallel to some line of array sensor. The 3-lines of approximately equally-spaced sensors used in this study is illustrated as arms in Figure III-1. The resulting $\vec{K}$-line spectra for each line gives the power density of the ambient noise as a function of its apparent wavenumber along that line. A more detailed discussion of the $\vec{K}$-line spectral technique has been published in a special report on $\vec{K}$-line spectral analysis using the TFO cross-array.*

The basic input data for calculating the $\vec{K}$-line spectra in the crosspower matrix, $\left[N_{ij}(f) \right]$, where f is frequency and i and j range over the sensors along the line. The crosspower matrix developed in Section III for the entire extended array was used to obtain such a matrix for each line of sensors. The matrix from all parallel lines of sensor were averaged to obtain a single matrix for each of three directions for which a $\vec{K}$-line spectra were computed. The average matrix was then normalized so that the main diagonal elements were unity.

The approximate spacing of the sensors forming the lines was 5 kilometers. The resulting foldover wavenumber of the spectra was .1 cycles/km.

The $\vec{K}$-line spectra computed for the three lines from all the matrices generated from the 'winter' and 'summer' data in the frequency band .1 to .5 Hz are in Figure IV-16 and IV-17 respectively. Each plot consists

---

* Array Research, Analysis of K-line Wavenumber Spectra from the TFO Long-Noise Sample, Special Report No. 23.

of a wavenumber power density spectrum, an integrated wavenumber power density function, and a discrete function marked by X's which show the fractional part that is unpredictable during an attempt to predict the output of the next sensor in a line from that of the preceding ones of the line. The 0-db level of the right hand scale for the power density spectrum is the average value of the spectrum. The fractional scale for the integrated spectra and the prediction error is on the right hand side. Two sets of vertical dashed lines are shown to indicate the approximate velocity of surface mode energy either traveling along the line or isotropic in nature (outer set) and to show the minimum apparent velocity, of p-wave noise (inner set). The inner set of vertical lines are not to be confused as an envelope for p-wave energy since directional surface mode energy could also fall inside them depending on the angle of incidence of this energy to the line of sensors.

A simultaneous analysis of the three $\vec{K}$-line spectra at each frequency confirms the spacial organization of the ambient noise previously observed in the 2-dimensional wavenumber analysis. The complexity and higher prediction of the 'winter' spectra compared to the 'summer' spectra is due to the multiple noise sources in the 'winter' sample as previously described.

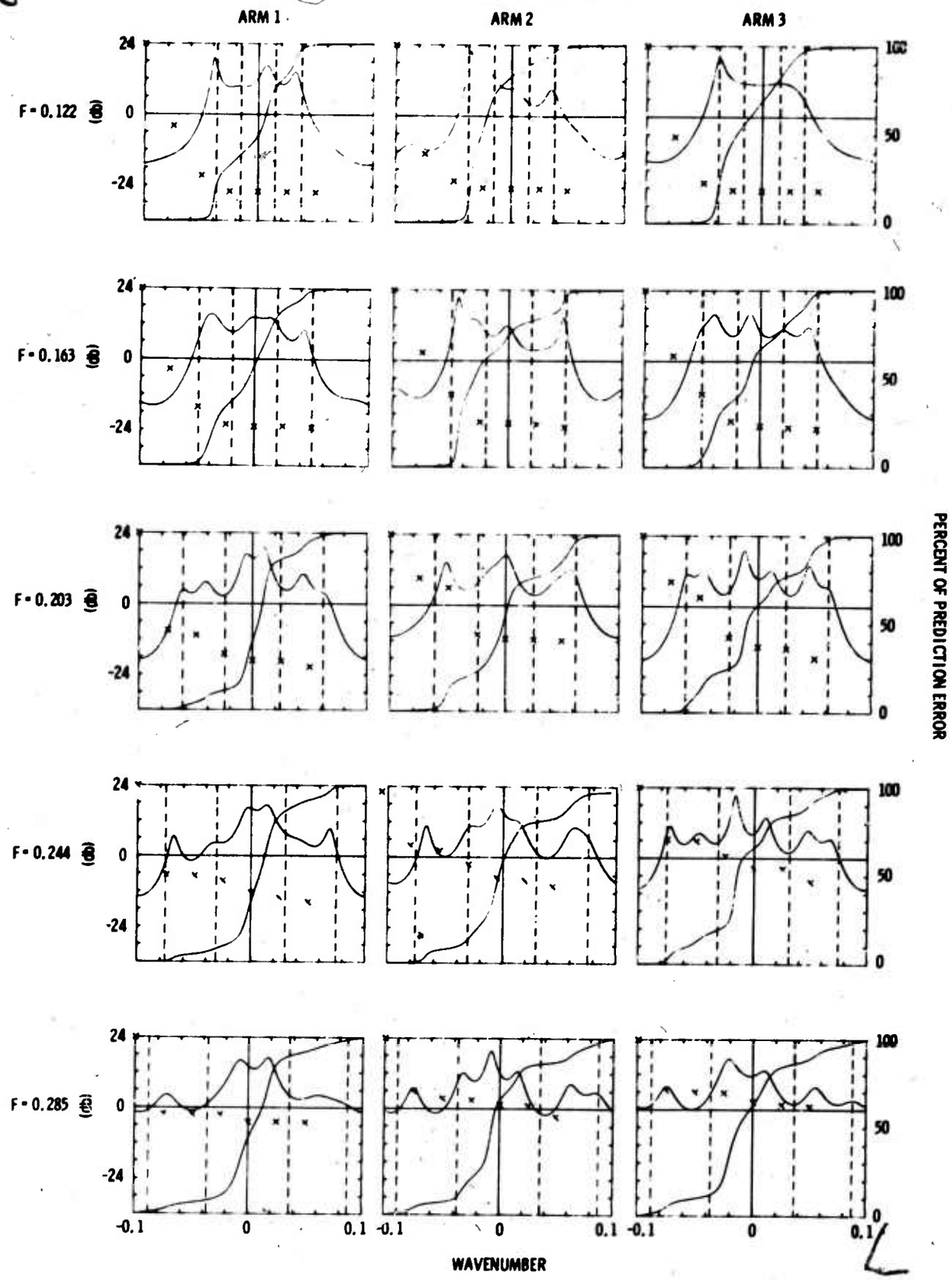

Figure IV-16. K-Line and Integrated Spectra of 'winter' Data Recorded from the Extended Short-Period Array

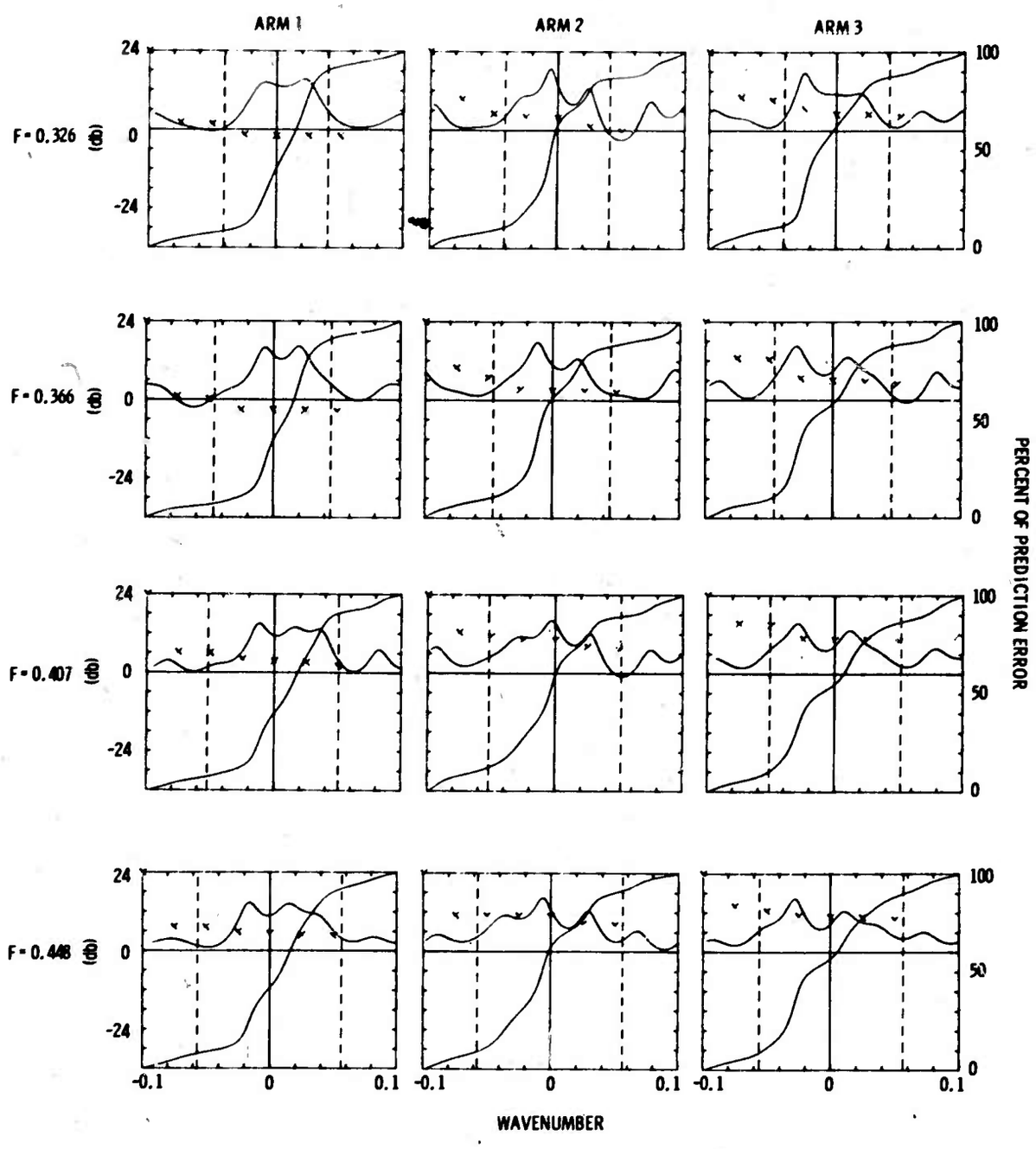

Figure IV-16 (Cont'd)

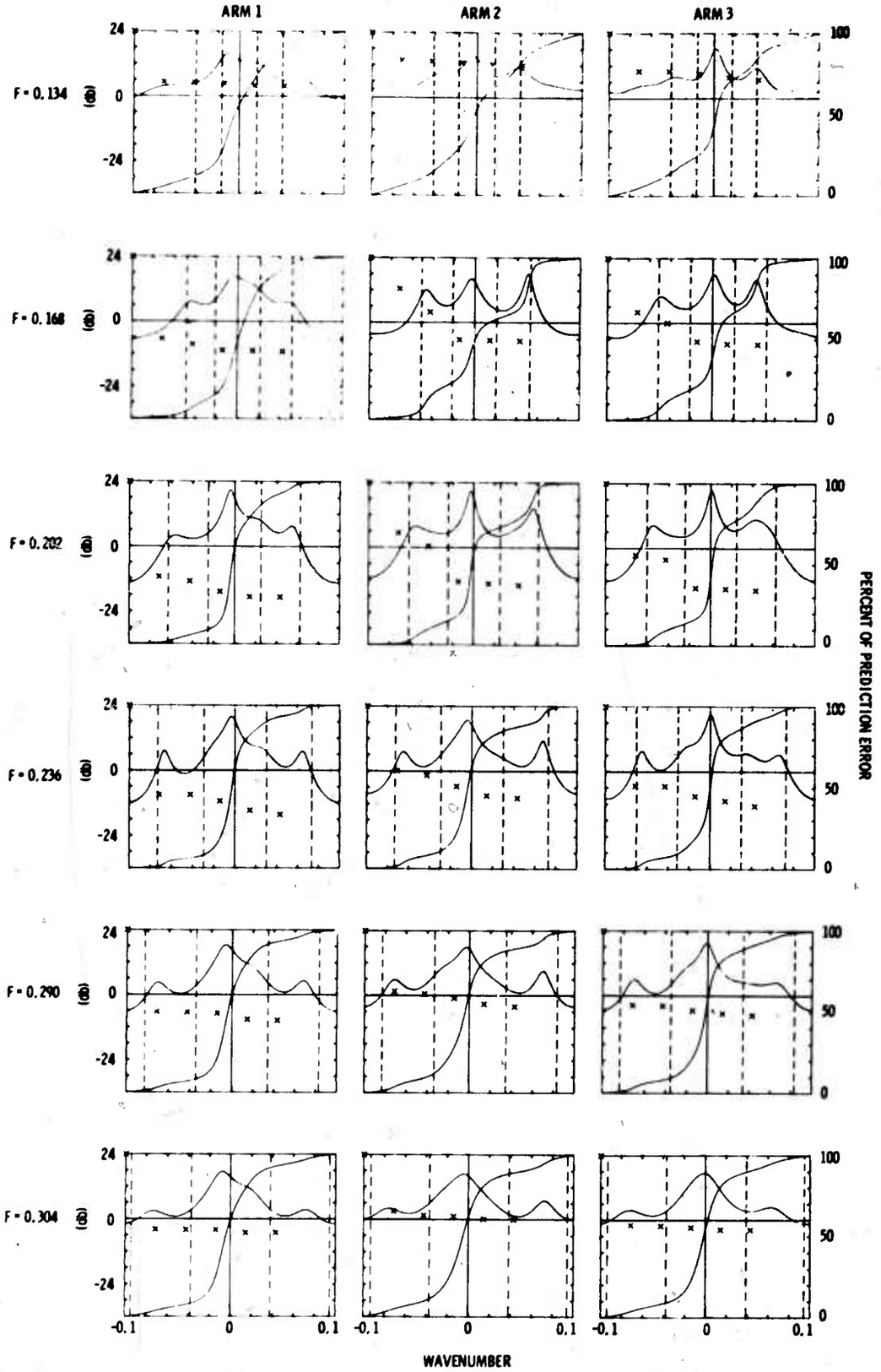

Figure IV-17. K-Line and Integrated Spectra of 'summer' Data from the Extended TFO Array

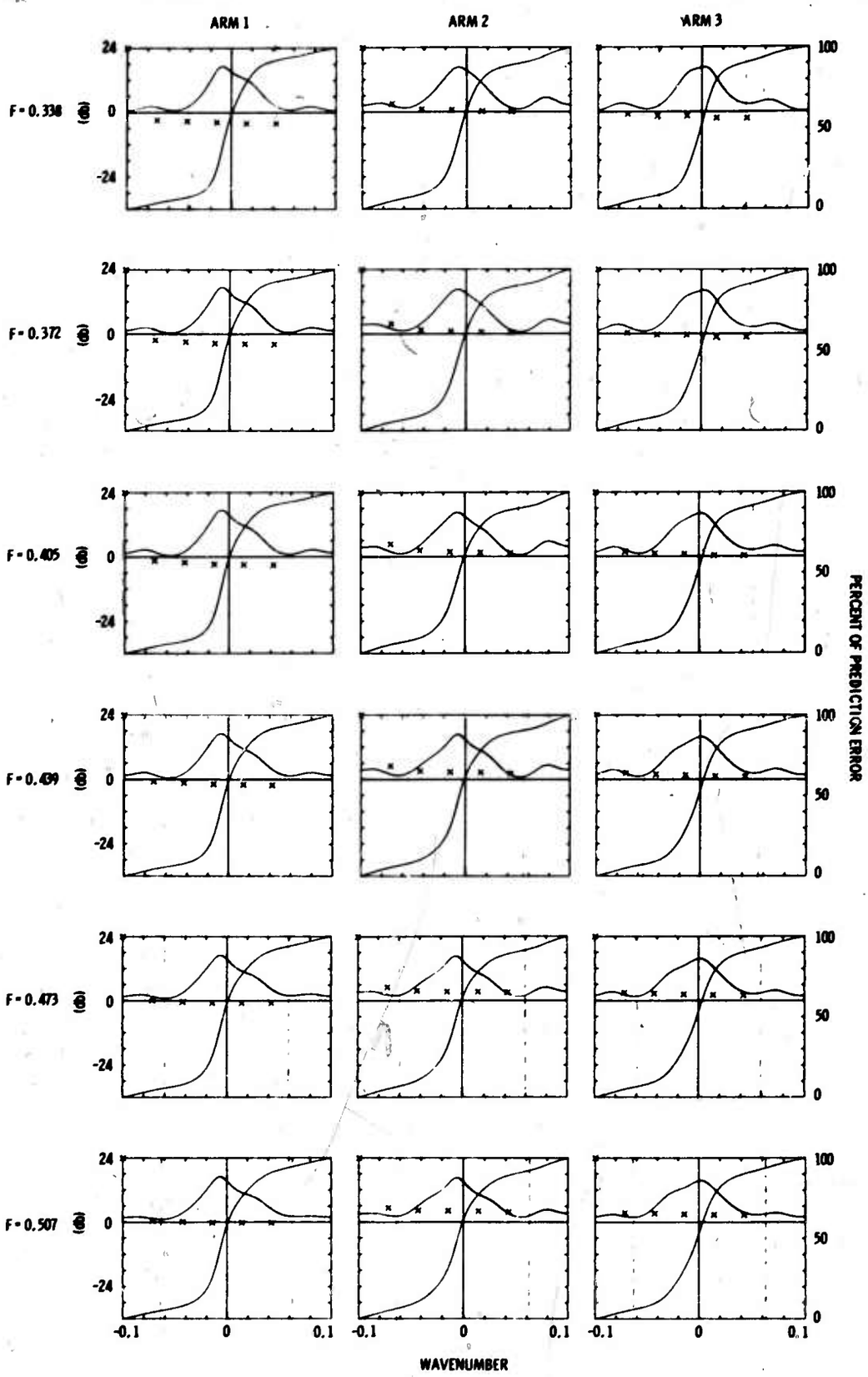

Figure IV-17. (Cont'd)

In the previous analysis, the direction of several definite contributors to the ambient noise field could be determined. The integraded wavenumber power density function was used in this study to estimate more accurately as a function of frequency the percentage each contribution is making to the total 'summer' and 'winter' noise level. The contributors considered consist of 4 directional surface mode sources, isotropic surface mode, and P-wave as illustrated in left most part of Figure IV-18. The P-wave contribution consists of any coherent energy with an apparent velocity of 8 km/sec or greater and would be contained inside the 8 km/sec circle of the wavenumber space represented by the figure. The surface mode contributors would be represented in wavenumber space along the circle representing the surface mode velocity of 3.2 km/sec. The percent of the total noise field which each contributed in the two noise samples analyzed are illustrated on the right of Figure IV-18. The most significant difference observed between the two noise samples is the large percentage of surface mode energy in the 'winter' noise at frequencies below .24 Hz. This appears to be primarily due to the energy from the direction of the Alaskan storm velocity previously discussed which significantly increases at lower frequencies. Such a generating source of noise should be of significant concern for longer period analysis since the percent of contribution is rapidly increasing for the longer-period energy. A similar observation can be made of the surface-mode energy from the South.

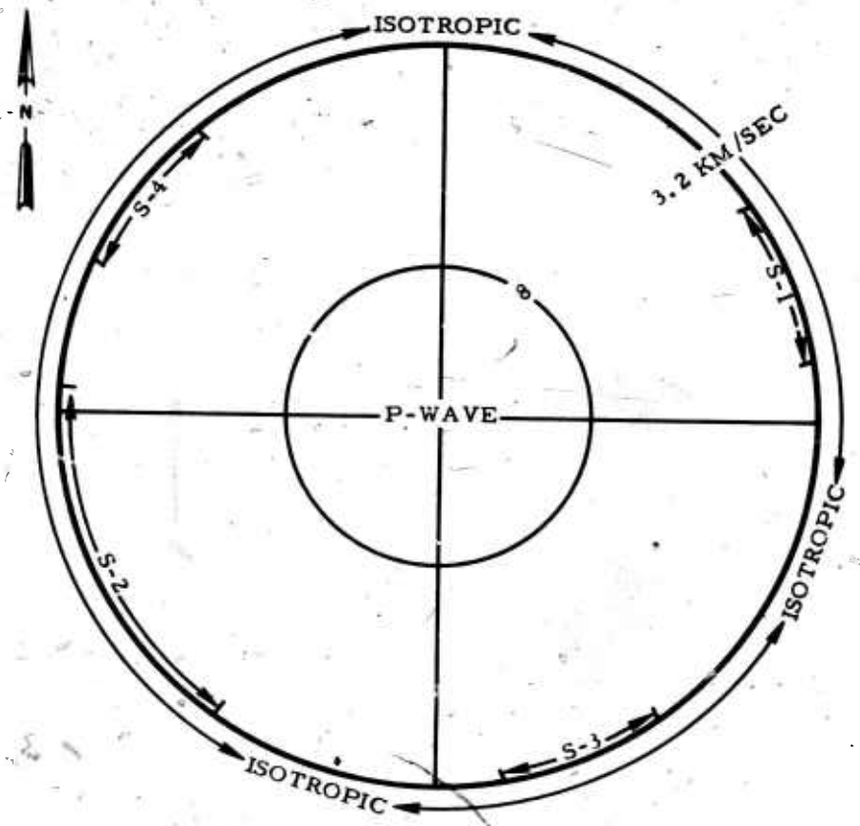

ILLUSTRATION C WAVENUMBER SPACE REFERENCED FOR EACH PRINCIPLE CONTRIBUTOR

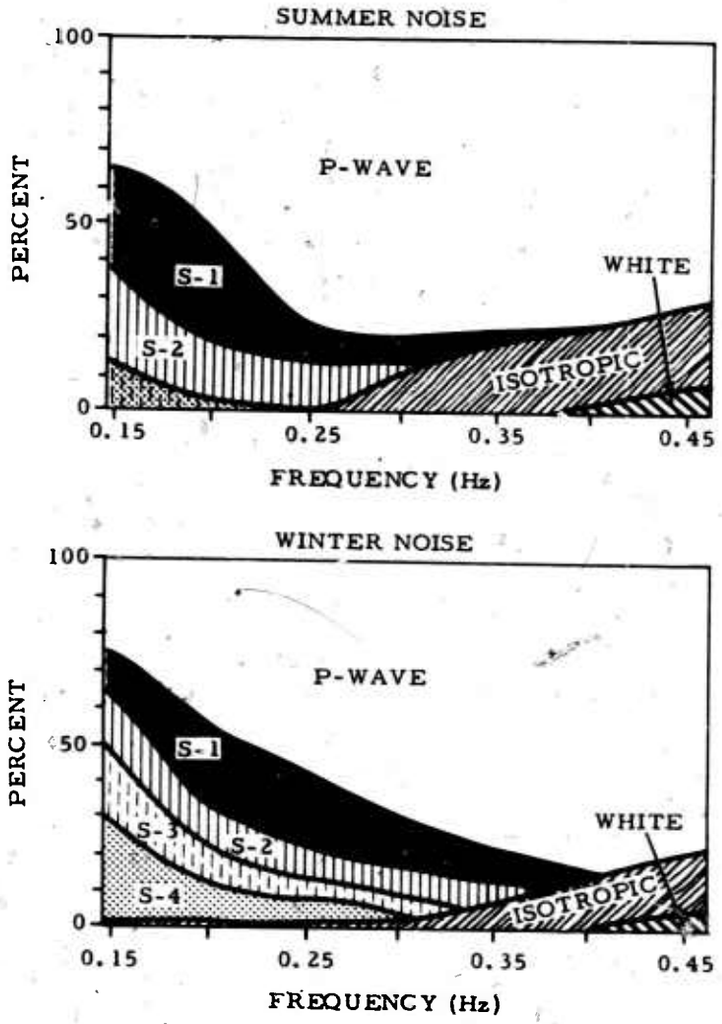

Figure IV-18. Distribution of Ambient Noise Power for Identified Sources

SECTION V
MULTICHANNEL FILTER DESIGN AND EVALUATION

The desirability of multichannel filtering for the extended short period array was determined by designing and evaluating signal extraction filters from the crosspower matrices developed in Section III. The performance of the multichannel filters were compared to that of the simple beam-steering process.

A. MCF DESIGN

A set of optimum Weiner multichannel filters were designed in the frequency domain from each of the generated crosspower matrices developed for the 'winter' and 'summer' data. The set of MCFs from the 'winter' data, denoted as MCF W, consist of 3 MCF designs, each using a subset of the 34 array elements. The first 'Winter' MCF (MCF W-7) was designed on the seven center elements (center seismometer Z1) plus the intermost ring of seismometers) of the extended array. MCF W-18 was designed on the same elements as MCF W-7 plus 11 elements of the next ring of sensors (sensors Z19 and Z22 were not operating properly). The third MCF, MCF W-34, includes all of the elements, except Z19, Z22, and Z31.

An equivalent set of MCFs developed from the 'summer' data is denoted as MCF S-6, MCF S-17, and MCF S-33. In this case only 6, 17, and 33 elements respectively were used due to one of the elements (Z-6) on the inner ring being bad. Figure III-1 is shown to indicate the elements actually used in each of the designs.

The signal model used in the MCF designs represented waves vertically incident to the extended array. The signal amplitude on each channel was assumed to have a constant ratio (1) to the noise on that channel at each frequency. The signal vector $\vec{V}$, is thus defined such $\nu_i = \sqrt{N_{ii}}$ where N_{ii} is an element of the noise crosspower matrix, N. The signal matrix is defined as $S = \vec{V}\ \vec{V}^H$.

The equation for the Wiener filter responses, $\vec{Z}$, to enhance the signal with minimum mean square error,

$$[N + S]\ \vec{Z} = (s/n)\ \vec{V} \quad \text{where } (s/n) = 4.0,$$

was solved at each of the desired frequencies.

B. EVALUATION OF MCFs

The designed MCFs were evaluated in the frequency domain through direct applications of the filter response, $\vec{Z}$, to the noise matrix from which they were designed and through an analysis of wavenumber responses at selected frequencies. The S/N improvement obtained in the application was compared to that obtained by simple beamsteering on the same data.

1. Signal-to-Noise Improvements

The signal-to-noise improvement for each of the MCFs was obtained by taking ratio of the output signal-to-noise ratio, S_o/N_o, where

$$S_o = \left| V^T Z \right|^2, \text{ and}$$

$$N_o = Z^{*T} N Z, \text{ to the input signal-to-noise ratio, } S_i/N_i,$$

where

$$S_i/N_i = 1.$$

The signal-to-noise improvement for the set of 'winter' and 'summer' MCFs is presented in Figure V-1 for the frequency band of 0.0 to 1.25 Hz. A comparison of the two sets show that the MCF W filters obtain a significantly higher S/N improvement below 0.75 Hz than the equivalent MCF S filters, as expected due to the previously observed increase of surface mode energy in the 'winter' data sample. A maximum of 11 db more S/N improvement was obtained by MCF W-34 than by MCF S-33 at the frequency of 0.12 Hz.

Similarly, S/N improvements were obtained for a straight summation process on each of the subset of elements. A ratio of the MCF improvement to this summation process is shown in Figure V-2. On the

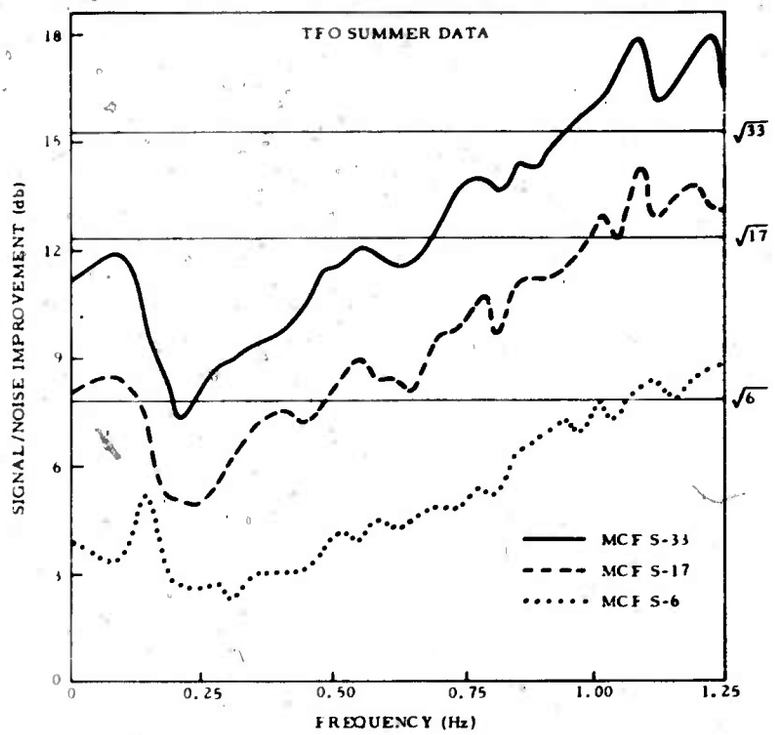

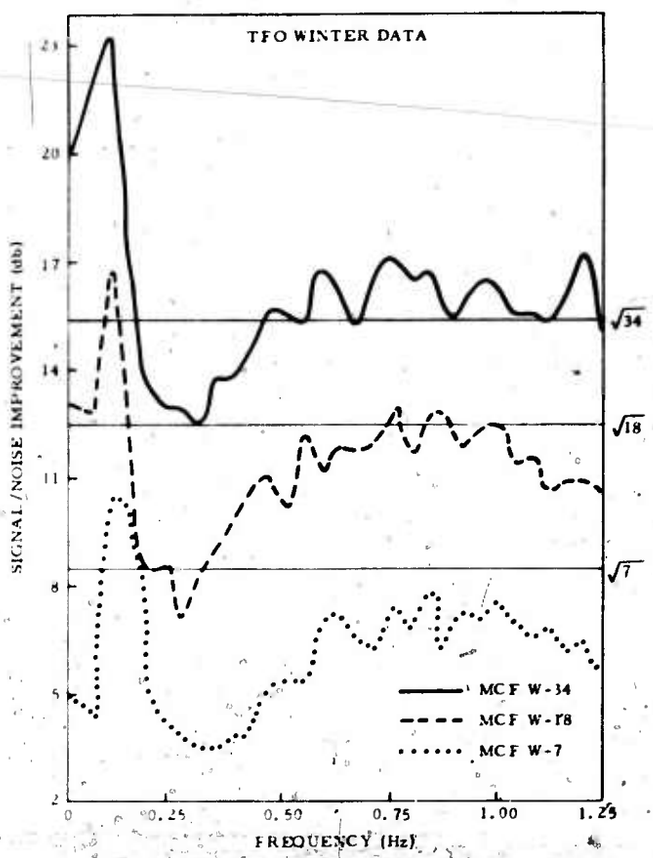

Figure V-1. Signal-to-Noise Improvement Obtained by MCF Processing on 'summer' and 'winter' Data

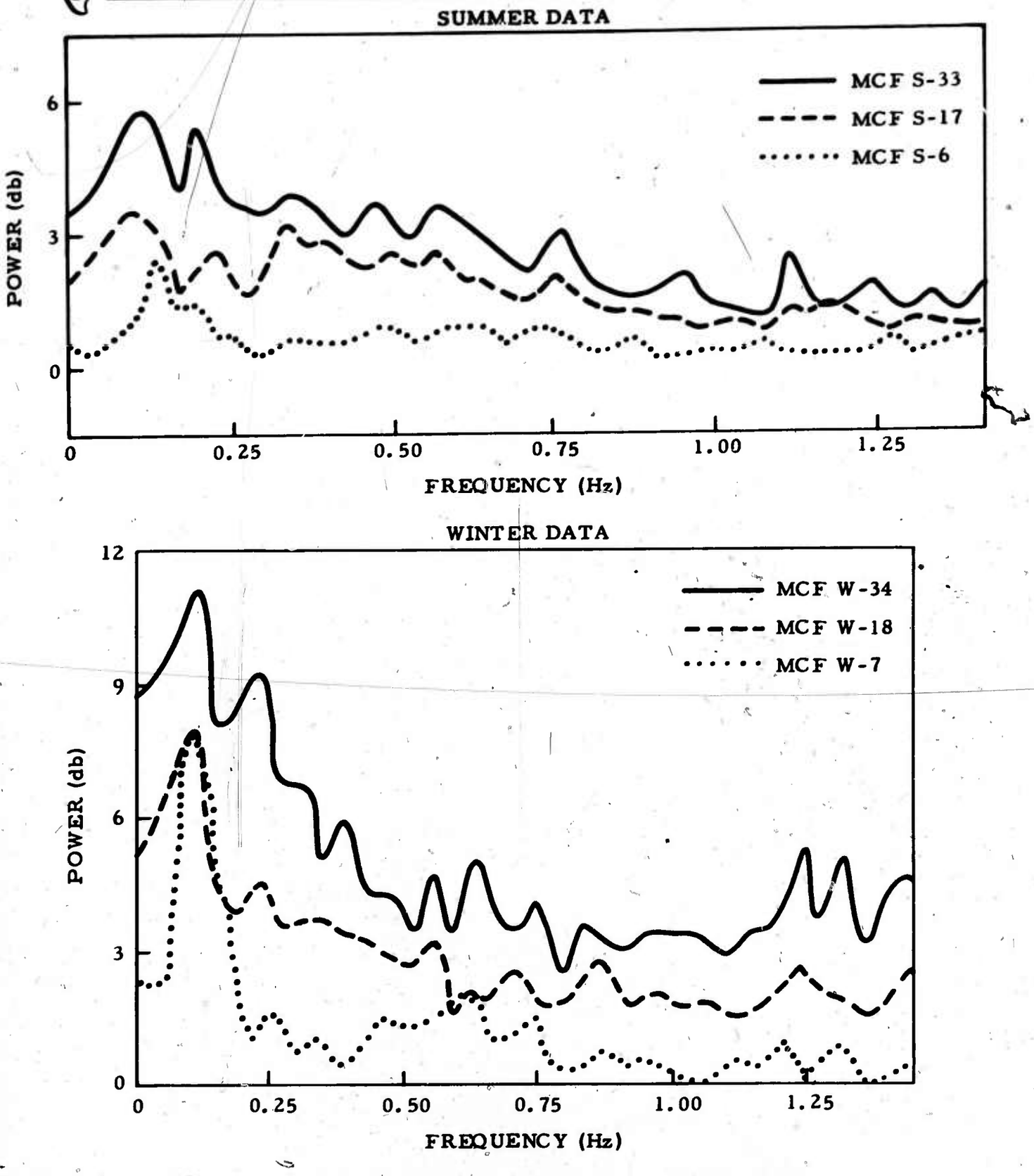

Figure V-2. Signal-to-Noise Improvement of MCFs Relative to Beamsteer Processing of Similar Elements

'summer' data less than 2.0 db gain is obtained by MCF processing at frequencies higher than 0.8 Hz. A maximum of 5.6 db S/N improvement over a summation process was obtained at 0.12 Hz by the MCF S-33. The MCF W set of filters show significantly more improvement over the summation. This is due primarily to the surface mode energy, however, since less statistics were used in the 'winter' sample than the 'summer' data some of the gain is false due to overdesign of the MCF. Based on a study by John Burg, et al,* results from evaluating the 34 channel filter MCF W-34 on the statistics from which it was designed will be biased approximately 1.4 db over the true optimum Wiener filter performance. (122 samples, 34 channels). For the 18 channel case, MCF W-18 the evaluation will be biased only .75 db. For the 'summer' data 230 effective segments of data was used to generate the matrices, thereby resulting in a 33 channel MCF with a bias of less than .7 db relative to the Wiener with the true filter.

Allowing for the false gain of the MCFs, the improvement at higher frequencies (above .75 Hz) is insignificant and a simple summation process is considered adequate. The improvement obtained in the .12 to .75 Hz band is directly related to the increase in the surface mode noise power of the noise sample.

C. WAVENUMBER ANALYSIS OF MCF RESPONSES

The wavenumber response of the MCFs, MCF W-34 and MCF S-33, were computed at several selected frequencies for comparison to the wavenumber spectra of the noise previously discussed in Section IV.

---

* Statistics Governing the Design and Performance of Noise-Prediction Filters, Advanced Array Research Special Report No. 3, 8 September 1967.

The wavenumber response of MCF S-33, at the lower frequencies of .135 and .169 Hz showing the k-space area being significantly rejected is presented in Figure V-3. Response at the signal region (K=0) is approximately .0 db. A dashed circle in the spectra represents surface mode values. Primarily the MCF is working to reject the surface mode energy from the Northeast and the West-Southwest with some emphasis placed on rejecting the p-wave energy coming from the South. There are also indications that the MCF is attempting to reject surface mode energy from the direction of the Gulf of Mexico to the Southeast of the array.

At two higher frequencies of .24 and .30 Hz (Figure V-4) the response becomes isotropic to surface mode velocities with some emphasis on the energy from the Southwest. The MCF continues to reject the p-wave energy from the South-Southwest. The velocity of 16 km/second from the Southwest is strongly rejected by the MCF at .304 Hz.

Comparable wavenumber responses for the MCF W-34 is shown in Figure V-5. At .122 Hz the MCF is strongly rejecting the surface mode energy from the Northwest and Southeast to obtain the 23 db signal-to-noise improvement of Figure V-1. As the frequency is increased to .244 Hz, the MCF begins to significantly reject the p-wave energy from the Northwest in addition to isotropic rejection of surface mode energy. At higher frequencies the MCF rejection of p-wave energy also becomes isotropic.

The significant difference in the 'winter' and 'summer' MCF is the rejection of surface mode energy from the Northwest at low frequencies (.12 to .24 Hz) and a more isotropic p-wave response at higher frequencies (.3 to .4 Hz).

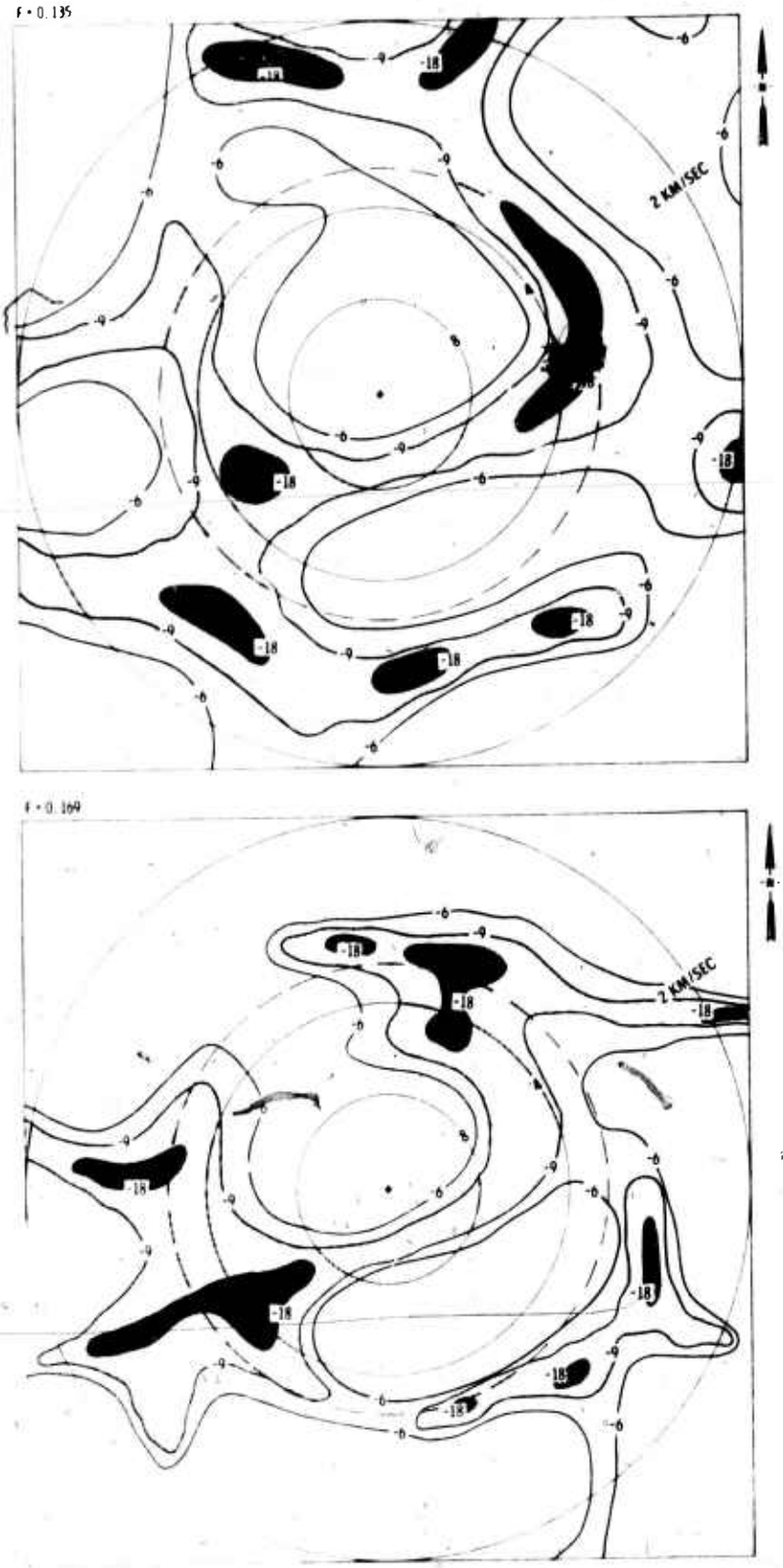

Figure V-3. Wavenumber Response of 'summer' MCF at Frequencies of .135 and .169 Hz.

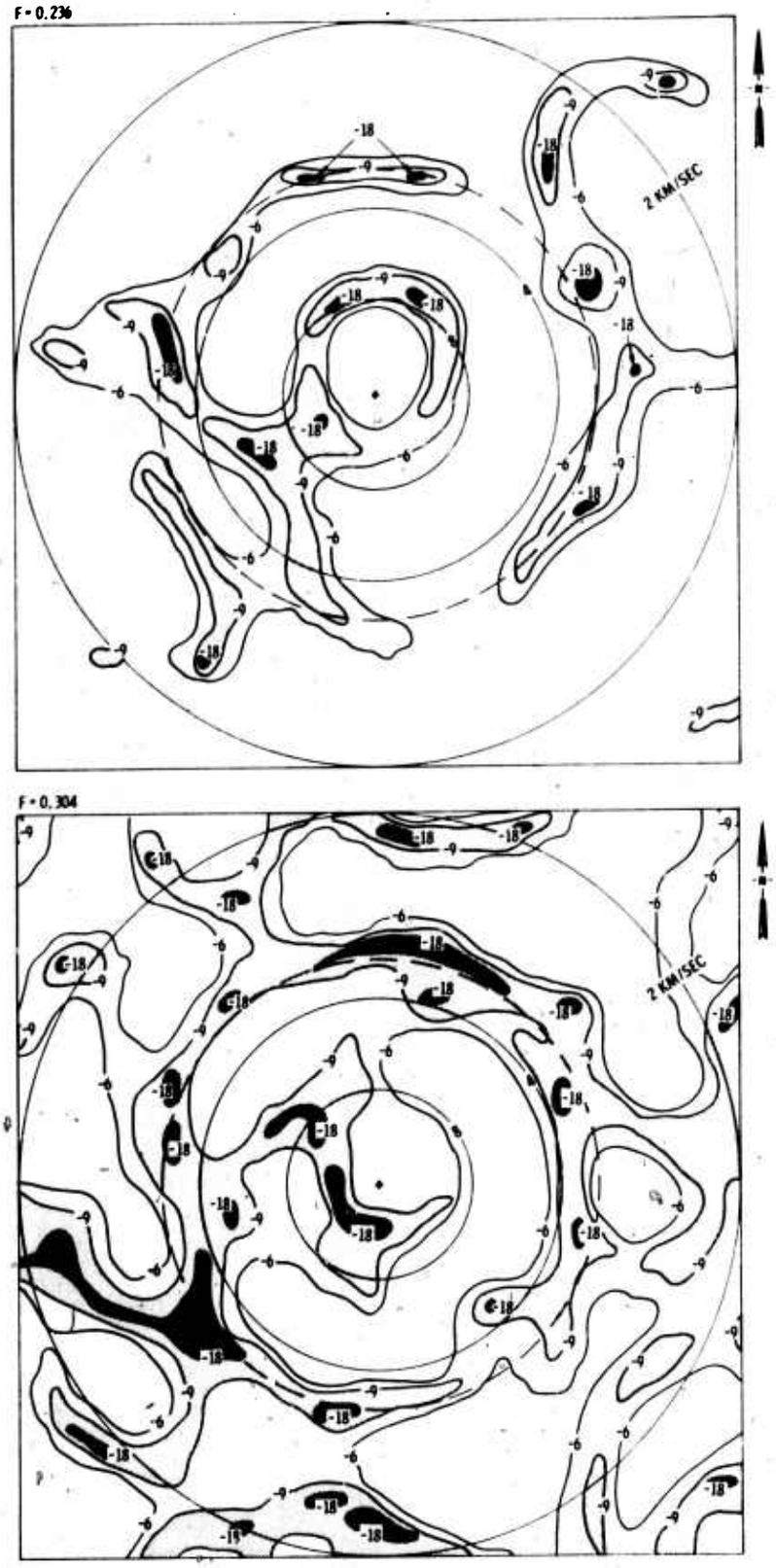

Figure V-4. Wavenumber Response of 'summer' MCF of .236 and .304 Hz.

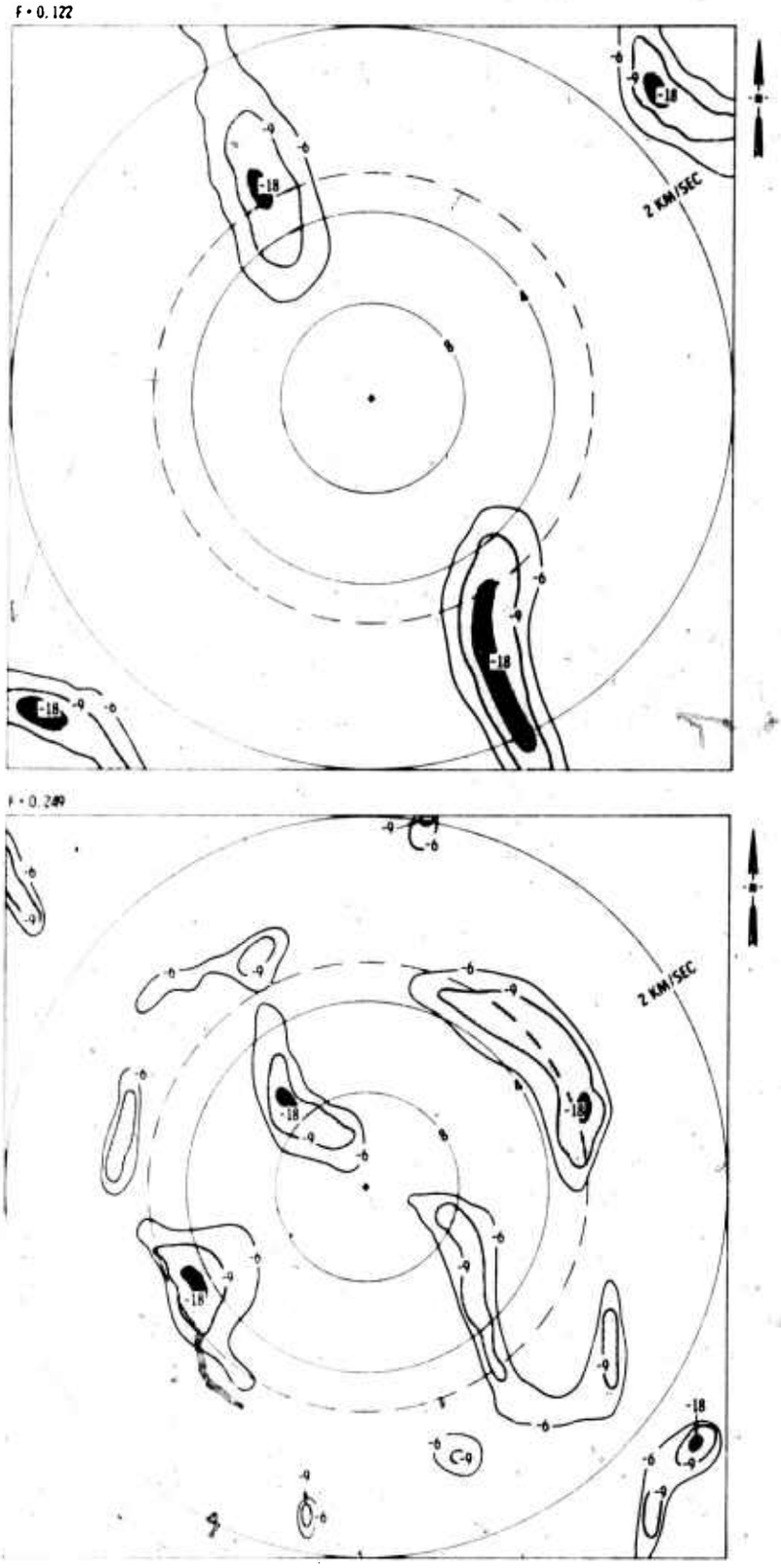

Figure V-5. Wavenumber Response of 'winter' MCF at Frequencies of .122 and .249 Hz.

D. CONCLUSIONS

The performance of multichannel filtering for the extended short-period array is highly dependent on the level of the noise. Under noisy conditions, apparently caused by storm activity near coastlines, MCFs can provide significant improvement over beamsteer processing at frequencies below .75 Hz. Above this frequency, however, very little improvement is obtained under either condition. Since the frequencies of prime signal interest lie in the higher frequency band and the generating sources, below .75 Hz are not stationary, the designed MCFs would not be useful for on-line application.

UNCLASSIFIED
Security Classification

DOCUMENT CONTROL DATA - R & D

Security classification of title, body of abstract and indexing annotation must be entered when the overall report is classified)

1. ORIGINATING ACTIVITY (Corporate author)
Texas Instruments Incorporated
Services Group
P.O. Box 5621, Dallas, Texas 75222

2a. REPORT SECURITY CLASSIFICATION
Unclassified

2b. GROUP
—

3. REPORT TITLE
NOISE STUDY FOR TFO EXTENDED SHORT-PERIOD ARRAY – SEISMIC ARRAY PROCESSING TECHNIQUES TECH. REPORT NO. 5

4. DESCRIPTIVE NOTES (Type of report and inclusive dates)
Technical

5. AUTHOR(S) (First name, middle initial, last name)
Thomas W. Rekieta

6. REPORT DATE
22 July 1970

7a. TOTAL NO OF PAGES
47

7b. NO OF REFS

8a. CONTRACT OR GRANT NO
F33657-70-C-0100

b. PROJECT NO
VELA/T/0701/B/ASD

9a. ORIGINATOR'S REPORT NUMBER(S)
—

9b. OTHER REPORT NO(S) (Any other numbers that may be assigned this report)
—

10. DISTRIBUTION STATEMENT
This document is subject to special export controls and each transmittal to foreign governments or foreign nationals may be made only with prior approval of Chief, AFTAC.

11. SUPPLEMENTARY NOTES
ARPA Order No. 624

12. SPONSORING MILITARY ACTIVITY
Advanced Research Projects Agency
Department of Defense
The Pentagon, Washington, D.C. 20301

13. ABSTRACT

Seismic data was digitally collected from the recently extended short-period array of the Tonto Forest Observatory during the summer of 1968 and the winter of 1969. An analysis of the data was made to characterize the ambient noise field from each period and to determine time-and space-stationarity of the fields. The effectiveness of multi-channel filter processing on the extended array was also measured.

Several contributors to the ambient noise field could be defined in both of the periods analyzed and appeared to be both time-and space stationary. Other contributors, due primarily to atmospheric storm or pressure activity, were not stationary and could be related to its generating source.

Multi-channel filtering of the extended array could not provide any significant improvement over simple beamsteering at frequencies of interest (greater than .8 Hz). At lower frequencies, the amount of improvement obtained by MCF processing relative to beamsteering was directly related to the increase in noise level due to the non-stationary contributor of the noise field.

DD FORM 1473

UNCLASSIFIED
Security Classification

14 KEY WORDS	LINK A		LINK B		LINK C	
	ROLE	WT	ROLE	WT	ROLE	WT
Seismic Array Processing						
Multichannel Filtering						
TFO						

END